UNIVERSIDADE D
COIMBRA

Adriana Filipa Ribeiro Carneiro

CIRCULATING TUMOUR CELLS: PAVING THE WAY TOWARDS THE IDENTIFICATION OF EPITHELIAL AND MESENCHYMAL PHENOTYPES IN THE CLINIC

Dissertação no âmbito do Mestrado em Biotecnologia Farmacêutica orientada pelo Professor Doutor João Nuno Moreira e pelo Doutor Luís Lima e apresentada Faculdade de Farmácia da Universidade de Coimbra.

Outubro de 2020

Faculdade de Farmácia da Universidade de Coimbra

Circulating Tumour Cells: Paving the Way Towards the Identification of Epithelial and Mesenchymal Phenotypes in the Clinic

Adriana Filipa Ribeiro Carneiro

Dissertação de mestrado no âmbito do Mestrado em Biotecnologia Farmacêutica, orientada pelo Senhor Professor Doutor João Nuno Moreira, pelo Doutor Luís Lima e pela Doutra Lorena Diéguez e apresentada à Faculdade de Farmácia da Universidade de Coimbra.

Outubro de 2020

1 2 9 0

UNIVERSIDADE D
COIMBRA

"Challenges are what makes life interesting and overcoming them is what makes life meaningful"

Joshua J. Marine

Acknowledgements

I started this year very hopeful, always believing that determination, inspiration and motivation are the key to achieve great success. Today, I am very grateful for the choices I have made, that led me to this particular moment and for the support and assistance that I received during this year.

I would first like to thank my supervisor, Professor João Nuno Moreira, at Universidade de Coimbra for all the guidance and patience during this year.

I would also like to express my sincere thanks to my supervisor at IPO do Porto, Dr. Luís Lima, for introducing me this wonderful project and for always being very supportive and encouraging at every moment.

In addition, I would like to acknowledge Dra. Lorena Diéguez, whose expertise was invaluable in formulating the research questions and methodology, for accepting me in her team and giving me the opportunity to develop my research and writing skills.

My deepest thank to all the INL team, for the excellent and enriching professional opportunity, but particularly to Paulina Piairo. Your insightful feedback pushed me to sharpen my thinking and brought my work to a higher level. Without your careful guidance, none of this would be possible. But, most of all I thank you for always having the time to listen, the wisdom to advice and the patience for helping me being a better version of myself.

Furthermore, I would like to express my gratitude to Alexandra Teixeira from INL for the friendship and for always having the kindest words in the most stressful moments.

I would also like to thank my parents for giving me the opportunity to study and pursue all my ambitions and future expectations. To my mother I would like to thank all the valuable lessons and for always pushing me. To my dad a sincere thanks for always believing in me.

Last, but not least, I would like to acknowledge my friends for their wise counsel and sympathetic ears, particularly Pedro, for knowing me as no one does, for always being there even in my darkest moments. To you I thank all the right words, all the deepest conversations, but most of all I thank you for being part of my life.

Finally, I would like to thank all the healthy volunteers that participated in this study, without them this work wouldn't be possible at all.

Resumo

O cancro colorretal (CCR) é o terceiro cancro mais incidente e o segundo com maior taxa de mortalidade a nível mundial. A principal causa de morte nestes doentes continua a ser a metastização, cerca de 60% dos mesmos são diagnosticados numa fase mais avançada da doença (fase III e IV). Há, por essa razão, uma necessidade urgente no desenvolvimento de estratégias que permitam o diagnóstico precoce e monitorização da doença metastática em CCR. Nesta perspetiva, as células tumorais circulantes (CTCs), libertadas pelo tumor para a corrente sanguínea, revelaram ter um papel importante como ferramenta para o diagnóstico e monitorização em tempo real do cancro. Estas refletem a heterogeneidade tumoral e a evolução clonal, bem como o seu isolamento e análise podem ser efetuados repetidamente ao longo do tratamento, de forma fácil, rápida e minimamente invasiva. Assim, o desenvolvimento de tecnologias que permitam a aplicação destas células na prática clínica é imperativo quer para a deteção precoce de potenciais recidivas, quer para a monitorização atempada da resposta do paciente ao tratamento. Este estudo teve como objetivo avaliar a eficiência de captura de um dispositivo de microfluídica, o RUBYchip™, desenvolvido no International Iberian Nanotechnology Laboratory (INL) com o propósito de capturar e caracterizar CTCs com base em duas características, o tamanho e a deformabilidade celular. A fim de otimizar o desempenho deste dispositivo, foram adicionadas concentrações definidas de células de diferentes linhas celulares de CCR (SW480, Caco2, RKO e HT-29) a 7,5 ml de sangue de voluntários saudáveis para posterior processamento a diferentes velocidades de fluxo de modo a aferir a eficiência de captura nestes tipos celulares. Posteriormente, a identificação e análise fenotípica de CTCs no RUBYchip™ foi efetuada por ensaios de imunocitoquímica com anticorpos que reconhecem a Citoqueratina, para uma seleção positiva dos CTCs; a Vimentina, expressa por CTCs em transição epitélio mesenquimatosa; e ainda, o CD45, para identificar e excluir as populações de células sanguíneas.

Após otimização, as condições ótimas definidas foram aplicadas em amostras de sangue periférico de pacientes recrutados no Instituto Português de Oncologia do Porto, com o propósito de identificar subpopulações de CTCs, que potencialmente podem predizer diferentes respostas clínicas.

Abstract

Colorectal cancer (CRC) is the third most commonly diagnosed cancer and the second with highest mortality worldwide. Metastases are the main cause of cancer-related mortality and 60% of patients are diagnosed at stages III and IV. Hence, there is an urgent need for the development of methodologies for the early diagnosis and monitoring of metastatic disease in colorectal cancer.

Circulating tumour cells (CTC) are shed from tumours into the bloodstream and are emerging as a fundamental tool for cancer diagnosis and monitoring. Just like solid tumours, CTCs are very heterogeneous, hence reflecting tumour heterogeneity and clonal evolution of cancer in real time. Adopting CTCs into the clinical practice, particularly in CRC, is imperative for early detection of potential recurrences, and in individualized monitoring of the disease during treatment. However, current tools in the clinic have shown limited sensitivity and clinical utility.

To overcome this limitation, a microfluidic technology for unbiased CTC isolation and characterization was developed at INL, the RUBYchip™, designed to capture CTC based on two important characteristics, cellular size and deformability. To optimize the performance of the device, four CRC cell lines (SW480, Caco2, RKO and HT-29) were spiked into 7.5 mL of healthy whole blood samples and processed at different flow rates to assess capture efficiency. Further identification and phenotypical analysis of CTCs in the microfluidic device was achieved by immunostaining with antibodies against Cytokeratin, to positively select CTCs; Vimentin, to identify CTCs that undergone epithelial-mesenchymal transition and CD45, to identify and exclude white blood cells.

Subsequently to optimization studies, whole blood samples from metastatic CRC patients, recruited at IPO do Porto, were processed in the microfluidic device and further analysed, aiming to elucidate and identify CTC subpopulations that could be related to different clinical outcomes.

List of abbreviations

AJCC American Joint Committee on Cancer

APC Adenomatous Polyposis Coli

BSA Bovine Serum Albumin

CEA Carcinoembryonic Antigen

CK Cytokeratin

CRC Colorectal Cancer

CTC Circulating Tumour Cell

DMEM Dulbecco´s Modified Eagle Medium

EGFR Epidermal Growth Factor Receptor

EMT Epithelial-Mesenchymal Transition

FAP Familial Adenomatous Polyposis

FBS Fetal Bovine Serum

FDA Food and Drug Administration

FIT Faecal Immunochemical Test

gFOBT Guaiac Faecal Occult Blood Test

ICC immunocytochemistry

INL International Iberian Nanotechnology Laboratory

IPO Instituto Português de Oncologia

LUT Lookup Table

MET Mesenchymal-Epithelial Transition

MMR Mismatch Repair System

MSI Microsatellite Instability

MSS Microsatellite Stable

OS Overall Survival

PBMC Peripheral Blood Mononuclear Cells

PBS Phosphate Buffer Saline

PDMS Polydimethylsiloxane Prepolymer

PFA Paraformaldehyde

PFS Progression Free Survival

VIM Vimentin

WBC White Blood Cells

TABLE OF CONTENTS

1. Introduction

1.1. Cancer: An Overview

The onset of cancer is believed to be a rare event as two different conditions, the deregulation of cell proliferation and the suppression of apoptosis, must take place together in the same cell. Otherwise, deregulated proliferation itself will ultimately cause cell death and, alternatively in the absence of cell proliferation, the suppression of apoptosis does not award any selective advantage[1].

Normal human cells are constantly growing and dividing to form new cells in order to replace old and defective ones and, at the same time, ensure the human body needs. But when there is a failure in this mechanism, cells that are already abnormal, old, or damaged continuing to grow uncontrollably, eventually forming growths called tumours. These malignant cells differ from normal cells; hence they can be distinguished under the microscope. Cancer cells are usually less differentiated and exhibit characteristics of rapidly growing cells such as a high nucleus-to-cytoplasm ratio, little specialized structure and, among others, a prominent nucleolus[2].

To better understand the biology of cancer, in 2000, Douglas Hanahan and Robert Weinberg proposed that as normal cells evolve to a neoplastic state, they would acquire a succession of characteristic traits that enable them to become tumorigenic, called the hallmarks of cancer[3]. These hallmarks were initially six, but about a decade later they were updated to ten major cancer hallmarks to include the contributions of tumour microenvironment to tumorigenesis, as illustrated in figure 1[4].

Although cancer complexity is simplified into specific cancer features that can be explained through mutations of characteristic cancer genes or interactions of genetic networks, the inclusion of these hallmarks into clinical practice (either in the diagnostic and treatment regimens) has failed because cancer is far more complex[5]. Indeed, these cancer marks help us to understand how cancer develops, but the scientific community is still far away from being able to answer why it happens in the first place.

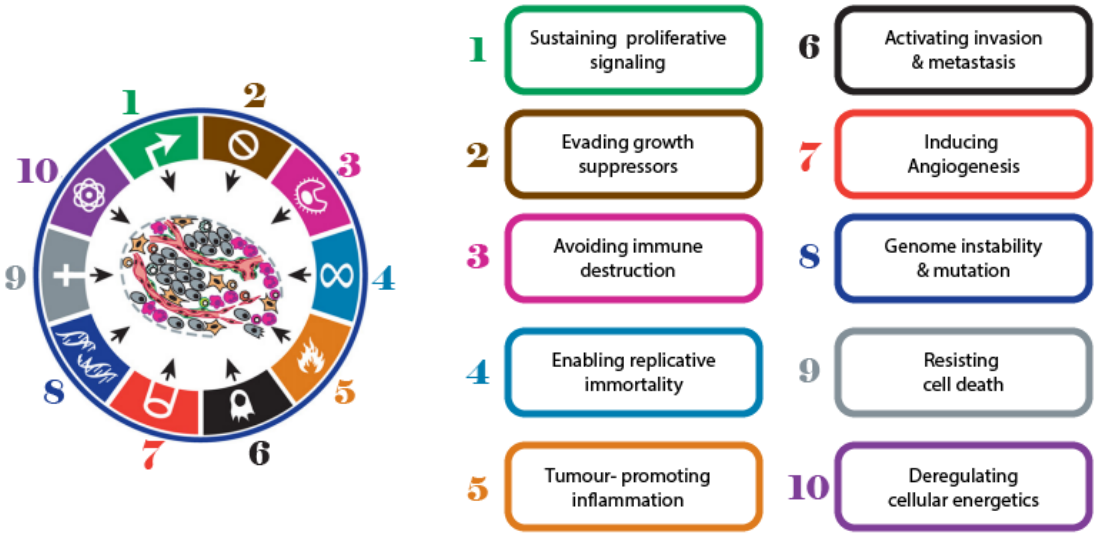

Figure 1: The Hallmarks of Cancer[4].

Cancer is a leading cause of morbidity and mortality worldwide, accounting to 9.6 million deaths in 2018. In-the same year the number of new cases reached 17 million globally and 58 199 in Portugal [6,7]. The International Agency for Research on Cancer reported that colorectal cancer (CRC) is a common type of cancer and the second with the highest mortality rate worldwide, outpaced only by liver cancer. In 2018, this malignancy was the second most common and the second with the highest death rate in Portugal[7].

1.2. Colorectal Cancer

Colorectum is constituted by the colon and the rectum, which combined are referred to as the large intestine. Together they form the final part of the gastrointestinal system and are mostly responsible for water absorption and solid waste excretion[8].

Although colon cancer and rectum cancer has been referred many times as one, there are some biological differences between one and the other based on the anatomical location [8]. One example of this is that tumours in the proximal colon are much more common in older patients than in younger individuals, and also more common in women than in men. Furthermore, patients with a tumour in the proximal colon have lower survival rates than those with tumours in the distal colon or rectum[9].

A diversity of risk factors is associated with this pathology, of which age is the main one since the risk of developing CRC is much higher after the fifth decade of life. Moreover, there are also increased risks associated with the family history and the existence of inflammatory bowel disease, characterised by chronic inflammation and abnormal cell growth or dysplasia[10].

Diet and lifestyle also have an impact on CRC development, as a low-fiber and high fat-diet with high consumption of red and processed meat has been associated to a higher risk of developing this pathology[11,12].

Late diagnosis is a major concerning issue in CRC, since many patients experience no symptoms in the early stages of the disease, depending on the tumour size and location in the large intestine. When symptoms eventually appear, it might be that metastasis has already occurred. Some of the most common symptoms of CRC are a persistent change in the bowel habits including diarrhea or constipation, or simply a change in the consistency of the faeces. Rectal bleeding or blood in the stool are also very common, and some patients also mention a persistent abdominal discomfort like pain or cramps[13]. An unexplained weight loss associated with weakness or fatigue could also be related to this disease especially when the patient also presented iron deficiency anaemia[13].

1.2.1. Colorectal Cancer Diagnosis and Screening

Nowadays there are several different types of screening and diagnostic tests that are used to detect colorectal cancer. Although some of these methods are invasive, they all have two important characteristics, sensitivity and specificity[14]. Current CRC screening tests can be differentiated, depending on their mode of action, between early detection tools or cancer-prevention tools[15].

Colonoscopy is considered the gold standard tool for CRC diagnosis, being the definitive examination strategy when screening tests are positive. Colonoscopy allows the direct visualisation of the entire large bowel, which makes it possible to directly detect and even resect both cancerous and precancerous lesions[16]. However, this technique is not only invasive, but also requires full bowel preparation and sedation during the procedure. Also, there is an associated risk of bowel perforation, along with post-colonoscopy bleeding. In addition, this methodology is expensive to be performed, so its potential application for mass screening is very questionable[14].

Flexible sigmoidoscopy has long been used for CRC screening. This methodology reliably detects colonic neoplasms in the distal colon and rectum. In comparison to the standard screening tool, the procedure time is shorter and there is often no need for sedation[17,18]. Additionally, there is no need for full bowel preparation and is less expensive. However, a number of studies have demonstrated that sigmoidoscopy may

miss a substantial portion of right-sided colonic neoplasia in patients without concurrent left-sided neoplasia[17].

Among the available screening strategies to detect CRC, Computed Tomography Colonography is a structural radiologic examination of the colon. Although this type of screening allows the identification of colonic lesions with lower procedural risks when compared to colonoscopy, it requires the same patient preparation and discomfort during procedure insufflation. Additionally, patients are also exposed to radiation and, in case of positive findings, have to be submitted to colonoscopy[14,16].

On the other hand, Guaiac Faecal Occult Blood Test (gFOBT) is a non-invasive, inexpensive, simple, and widely available screening test that aims to detect the presence of blood in faeces. Its methodology simply consists in an oxidation reaction dependent on the peroxidase activity of heme, a component of hemoglobin[16]. But this test requires a moderate quantity of heme to induce a reaction, hence lacks in sensitivity[14].

Like gFOBT, Faecal Immunochemical Test (FIT) detects blood on faeces, more specifically human globin through an antibody-based assay. This sampling technique is simple and easy to collect, requiring a smaller faecal sample when compared to gFOBT, and shows a greater sensitivity for detecting advanced adenomas and CRC[16].

More recently, in 2014, a new non-invasive, multitarget stool DNA screening test for CRC was approved by the Food and Drug Administration (FDA), the Cologuard. This stool DNA test has the ability to detect abnormal DNA and occult blood in stool samples[16], that the result of the test depends on a stipulated threshold of abnormal DNA and/or blood. In case of a positive result the patient would then be referred for a diagnostic colonoscopy, otherwise if the levels are below the threshold, the patient should continue with recommended routine screenings[14]. Cologuard holds a lot of potential since it does not require any bowel preparation or diet changes, has high sensitivity and is relatively cheap. However, some concerns still exist around this screening test, since it is still recent and has shown limited evidence[14].

A brief comparison of the explained CRC screening/diagnostic tests is summarized in table 1. In order to improve patients' health and reduce CRC mortality is imperative to increase patients' compliance with CRC screening. In that perspective, it is urgent to find cost-effective and non-invasive methodologies that reduce complications and anxiety over CRC screening and ultimately improve overall acceptance of the screening process[16].

Blood based markers emerge as a promising tool for CRC screening, however colonoscopy continues to be the standard methodology for diagnosis in individuals selected as high risk.

Table 1 *Comparison of Current Methods for Colorectal Cancer Screening.*

Modality		Sedation	Diet and medication changes before test?	Detection Sensitivity	Biopsy or Polypectomy	Bowel Preparation	Invasive Procedure	Test Frequency
Endoscopic	Colonoscopy	Usually	Yes	95%	Yes	Yes	Yes	Every 10 years
	Sigmoidoscopy	Rarely	Yes	95% Only left sided cancers	Yes	Yes (Less extensive than Colonoscopy)	Yes	Every 5-10 years
Stool Test	gFOBT	No	No	70%	No	No	No	Every year
	FIT	No	No	73.8%	No	No	No	Every year
	Cologuard	No	No	92%	No	No	No	Every 3 years
Radiologi	CT Colonography	No	No	88.8%	No	No	No	Every 5 years

1.2.2. Colorectal Cancer management: Staging

Once CRC is diagnosed, disease staging is performed according to the TNM System developed by the American Joint Committee on Cancer (AJCC), which is based on three main features, namely the size of the tumour (T), the spread to nearby lymph nodes (N) and the spread to distant sites or metastasis (M)[19], as detailed in figure 2.

Development of metastasis is a concern for patients and clinicians, as survival rates drastically decrease in a metastatic setting. Strikingly, approximately 60% of CRC patients already have metastasis at the time of the diagnosis, 35% with regional lymph nodes metastasis and 22% with distant metastasis[20,21]. With the help of continuous developments in CRC treatment, survival rates have improved, however patients with advanced disease at the time of the diagnosis have a 5-year relative survival of 14.3%, while at an early-stage the 5-year relative survival is 90.2%, so early detection is key for a good prognosis[20].

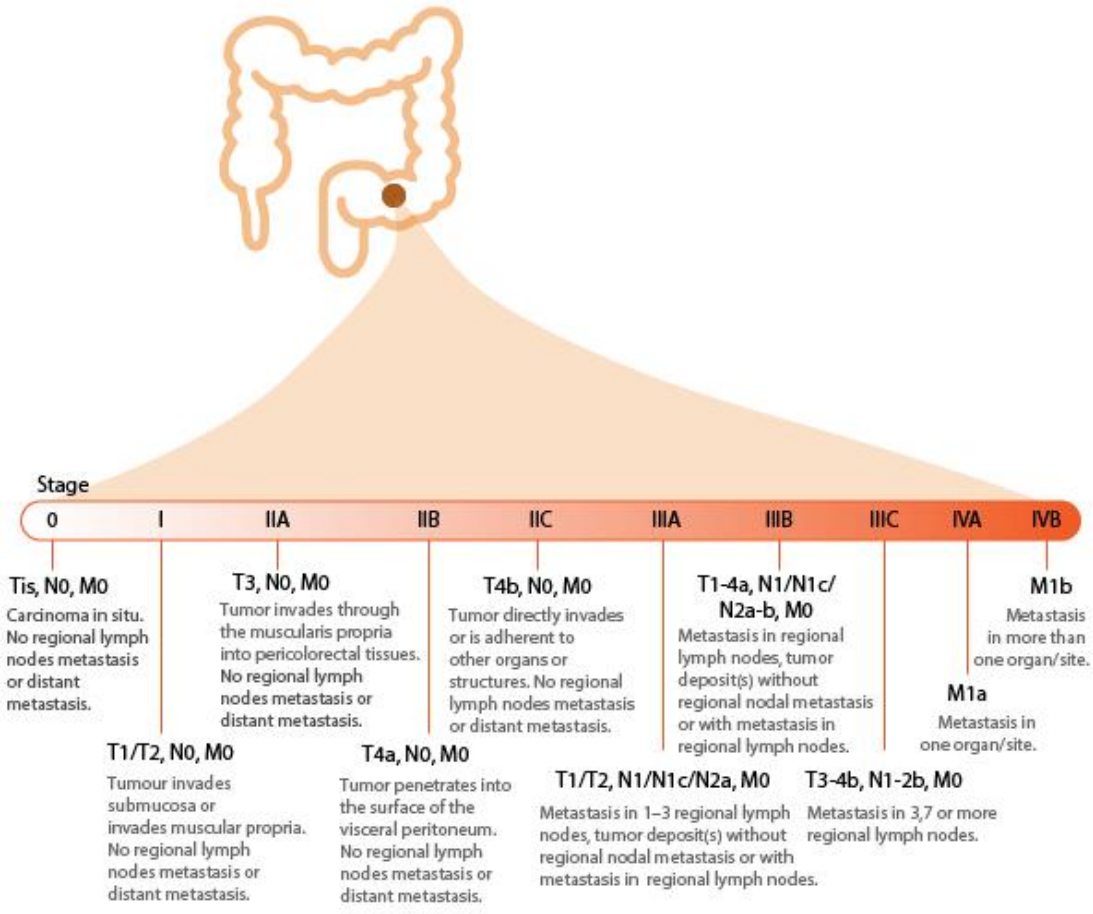

Figure 2: Anatomic Colorectal Cancer Stage according to the American Joint Committee on Cancer (AJCC)[20].

1.2.3. Molecular Overview in Colorectal Cancer

Colorectal cancer is a complicated disorder that is not a result of a single cause, but most of the times several mechanisms are involved in molecular tumours subtypes which have considerable prognostic implications.

Colorectal malignancies are classified as inherited and familial in about 30% of CRC cases, normally involving a familial component with a possible definable genetic basis[13]. This type of CRC is frequently associated to highly penetrant monogenic germline mutations, which highly confers lifetime risk of CRC development[22]. Familial CRC are divided in two groups, the polyposis and non-polyposis form. The main difference is that the polyposis form are related to *adenomatous polyposis coli (APC)* gene mutations and involves the formation of multiple potentially malignant polyps in the colon, while the non-polyposis is related to mutations in DNA repair mechanisms[23].

Familial Adenomatous Polyposis (FAP) is precisely characterised by the formation of hundreds of thousands of colonic adenomas at an early age in patients and without medical intervention it's likely that this person will develop CRC by the age of 40[22,23].

It is not known at what age the onset of colonic adenomas occur because is variable in each patient, but it is thought that at 10 years of age approximately 15 % of patients manifest adenomas, by the age of 20 the probability increases to 75 % and by the age of 30, 90 % will have presented with FAP[22]. In this syndrome, the *APC* gene, which is a tumour suppressor gene, is in most cases mutated and, is responsible for the classic polyposis phenotype.

However, the most common form of hereditary CRC is non-polyposis form, also known as Lynch Syndrome (LS). A germline mutation in genes associated with the DNA mismatch repair system (MMR) is responsible for this syndrome[22]. Tumours in this type of CRC are often poorly differentiated and presented an accelerated carcinogenesis. In fact, a small colonic adenoma may emerge as a carcinoma within 2 to 3 years when usually this process takes 8 to 10 years to occur in the general population[23].

Still, the most frequent type of CRC in the population is sporadic cancer, which results from point mutations that appear during life and, in spite of targeting different genes, in CRC about 70 % of the cases follow a specific succession of mutations resulting in the formation of an adenoma that fast evolves to a carcinoma state[10].

These mutations could appear in various genes with crucial functions within the cell driving to chromosomal instability (CIN), island methylator phenotype (CIMP) and microsatellite instability (MSI), which are the three main mechanisms in CRC onset[24]. According to several studies, in CIN pathway, the first mutation occurs in a tumour suppressor gene, the *APC* gene, followed by mutations in oncogenes like *KRAS* and inactivation of tumour suppressor genes such as *TP53*[24]. In addition, there is an increase of β-catenin levels which leads to the activation of the Wnt signalling pathway, important in functions like stem-cell differentiation and cellular growth. This altered pathway may drive tumour development because is associated with weakened tight junctions and therefore reduced cellular adhesion, favouring migration, and metastasis[25].

Furthermore, *KRAS* mutations leads to the increasing of RAS signalling which further activates the RAF-MEK-ERK and PI3K-AKT-PKB pathways or RAL small GTPases[24]. The activated PI3K are responsible for *AKT1* and *AKT2* genes activation, which enhances tumour growth by promoting epithelial-mesenchymal transition (EMT). The presence of this type of mutations are likely associated with poor prognosis as well as lower survival rates in CRC patients[13].

Another gene that appears to be affected in CRC patients is *PTEN*, a tumour suppressor gene that is activated under stress targeting cell cycle inhibitors and pro-

apoptotic factors. But, loss-of-function mutations in this gene may induce AKT-regulated metastasis in CRC[24]. Also, although not common, TGF-β pathway, crucial in cellular processes such as growth, differentiation, and apoptosis, is known to be deregulated in CRC[13].

Microsatellites are short repetitive DNA sequences positioned throughout the human genome, so the MSI could occur due to mistakes that do not get corrected during DNA replication because of inactivating mutations that occur in DNA *mismatch repair (MMR)* genes, responsible for correcting those DNA replication errors[24]. This dysregulation could be derived from germline mutations in the *MMR* genes- *MLH1, MLH2, MLH6* or *PMS2*- or could also be caused by sporadic mutations resulting in the inactivation of *MLH1*[26]. Based on the percentage of loci affected, microsatellite instability could be classified into microsatellite instability-high (MSI-H) or microsatellite instability- low (MSI-L). And in case of lack of MSI features the tumour is designated as microsatellite stable (MSS).

In addition to MSI with a sporadic origin is frequently associated a *BRAF V600E* mutation, which is extremely rare to occur in familial CRC cases like LS. So, *BRAF V600E* mutation analysis is frequently performed in order to distinguish sporadic from hereditary forms of CRC, as well as guide further germline mutations analysis[26]. MSI tumours occur in about 15 % of colorectal cancer patients and are normally more associated with proximal colon, as well as poor differentiation, but better prognosis for CRC patients who presented this type of abnormalities[24].

Another carcinogenesis mechanism involved in CRC is the CIMP pathway characterised by promoter hypermethylation which results in the transcriptional inactivation of genes that have tumour suppressor roles or are involved in the cell cycle, specially *MGMT* and *MLH1* [24].

Colorectal cancer is a complicated disorder that is not a result of a single cause, but most of the times several mechanisms are involved in molecular tumours subtypes which have considerable prognostic implications.

1.2.4. Biomarkers in Colorectal Cancer

Biomarkers are defined as any substance, structure or process that can be measured in the body or its products, allowing the understanding of the presence or progression of a specific disease or the effect of a particular treatment[10,27]. Thus, they need highly specific, sensitive and easy to be measured[10].

Regarding CRC there is an urgent need for new diagnostic and prognostic biomarkers, not only to decrease CRC mortality, but also to better predict disease evolution and to design the best treatment for each patient.

One of the earliest studied prognostic biomarkers in CRC and the main one used in the clinical practice is carcinoembryonic antigen (CEA), a glycoprotein expressed in colorectal malignancies[28]. This blood-based biomarker was firstly described as specific for CRC, but evidence showed that this protein can be expressed in other malignancies as well as in inflammatory conditions, such as inflammatory bowel disease. So, CEA may lack specificity that is why its expression levels must be interpreted with caution[29]. In general, elevated levels of CEA have been related to more aggressive types of cancer specially when found in stage II and III CRC patients. But could also be associated with cancer progression and indicative of recurrence disease particularly after surgery[30].

In terms of genes, the only one that has entered in the clinical practice routine was the study of *KRAS* in metastatic CRC patients receiving epidermal growth factor receptor (EGFR) targeted therapy[31]. The *KRAS* gene encodes a small GTPase transductor responsible for the regulation of cellular growth and differentiation and is involved in the RAF–MEK–ERK cascade, whose function is the transmission of signals from extracellular receptors to transcription factors [32]. Therefore, a mutation in this gene may result in the continuous activation of a signal transduction pathway which results in the inefficacy of therapy with anti-EGFR antibodies[31].

Regarding *BRAF* mutations, it has been described that they do not predict response to standard chemotherapy, however there are a number of studies that show a predictive value in the lack of response to anti-EGFR treatment. For this reason, it is assumed that this type of mutations may be used as a biomarker to screen CRC patients treated with anti-EGFR antibodies[31]. A comparison study between two groups of CRC patients, one with both wild type *KRAS* and *BRAF* (wt*KRAS*, wt*BRAF*) and another with wild type *KRAS*, but mutated *BRAF* (wt*KRAS*, mt*BRAF*), showed that both groups responded to Cetuximab, a monoclonal antibody used in EGFR target therapy. However, there was a better response from the (wt*KRAS*, wt*BRAF)* group of patients, while the group with (wt*KRAS*, mt*BRAF)* presented lower overall survival (OS) and progression free survival (PFS)[29].

Microsatellite instability is another genetic alteration that has been widely studied since it shows potential as a prognostic biomarker. Preclinical data has showed that CRC tumours with this type of genomic abnormalities tend to be 5-fluorouracil (5-FU) resistant, but sensitive to oxaliplatin, two anticancer drugs used in the colorectal cancer

treatment[26]. Moreover, retrospective studies and meta-analysis in stage II and III CRC patients exhibited that the MSI presence was a predictive factor of improved OS regardless the cancer stage. Besides, MSI-H patients also showed lower lymph node metastasis incidence and distant metastases when compared to MSI-L or MSS cancer cells, which is in overall associated with a better prognosis[30].

Prospective biomarker-driven studies are now under investigation to identify potential prognostic and predictive biomarkers for CRC screening and treatment. Cancer biomarkers hold the potential to provide non-invasive and cost-effective diagnosis, as well as to allow more rational use of medication with the ultimately goal of preventing patients from undergoing unnecessary ineffective treatments, avoiding their side-effects, and providing better use of health-care resources[30,33].

1.2.5. Epithelial- Mesenchymal transition and metastatic Colorectal Cancer

Epithelial cells are normally arranged in cohesive sheets mediated by several types of cell junctions to keep them attached to each other. But, sometimes under specific circumstances, epithelial cells are stimulated to undergo EMT, a biochemical shift that allows them to become mesenchymal. During this process, epithelial cells suffer multiple changes that enable them to become non-polarized elongated mesenchymal cells as they lose intracellular junctions and acquire the capacity to move through the extracellular matrix[34].

EMT could be related to different stimuli processes and, for that reason, this type of transition is classified into three distinct types. Type 1 is associated with implantation, embryo formation, and organ development in embryonic stage after fertilization. Type 2 is related with wound healing, tissue regeneration and organ fibrosis. Finally, type 3 occurs in cancer cells and, therefore is related to cancer progression and metastasis[35]. This last type of EMT is responsible for promoting fibroblastoid morphology, cell migration and invasion, resistance to apoptosis and chemotherapy, and also helps to maintain the overall cancer stem cell phenotype[36].

During this process, several changes occur at the molecular level, such as changes in the expression of genes and specific microRNAs, function and activation of various proteins. But they also occur at biochemical level since there is a metabolic reprogramming in those transitioned cells, which is characterized by upregulated

glycolysis, lipid metabolism, activation of the pentose phosphate pathway, and mitochondrial biogenesis, resulting in high energy production[36]. In addition, loss of adhesiveness is one of the most significant changes during EMT that is related with the downregulation of canonical epithelial markers, such as E-cadherin, cytokeratins, and ZO-1, and the simultaneous increase of expression of mesenchymal markers like N-cadherin, vimentin, fibronectin and α-SMA[37]. Other critical features associated with this transition mechanism are the production of extracellular matrix-degrading enzymes, the cytoskeleton reorganization and, ultimately the activation of transcription factors, for example Twist, Snail, Slug, ZEB, and β-catenin, that regulate EMT markers[36].

For colorectal cancer, some of these alterations may have a negative impact on the patient prognosis. For example, it has been shown that the loss of E-cadherin expression is associated with a poor prognosis in stage III CRC patients. Also associated with poor prognosis in CRC patients is the elevated levels of fibronectin, an extracellular protein required for mesenchymal cell migration[38]. Furthermore, evidences showed that overexpression of N-cadherin is related with metastasis poor survival rates [39]. Overall, aberrant regulation of EMT-related transcription factors, as well as mesenchymal markers seems to be correlated with increased rate of recurrence and decreased survival[38].

Being widely related to the metastatic cascade, EMT works as the very first step of this process by increasing invasiveness, allowing cells to migrate through the extracellular matrix and colonize in the lymph or blood vessels[38]. However, both metastatic process and EMT are highly complex cellular mechanisms regulated by a diverse of signalling molecules, transcription factors, epigenetic regulators, and non-coding RNAs, so it is not yet clear the precise mechanism that links both processes[40].

Advances in precision medicine have radically changed the therapeutic scenario in medical oncology. There is a constant searching for target therapies, which often relies on the presence of specific tumour biomarkers. However, in many cases, these biomarkers are not uniformly present in all cancer cells, and such heterogeneity has been implicated as a source of therapeutic resistance and treatment failure[41,42]. Furthermore, it has been reported that dynamic cell plasticity increases the phenotypic heterogeneity of tumours, hence tumour versatility at the population level. Such phenotypic plasticity could be acquired through epithelial-mesenchymal transition, which increases the complexity of the mechanisms underlying carcinogenesis, metastasis and its treatments[43]. Thus, there

is an urgent need for new technologies able to study single cell phenotypes and cell state transitions.

1.3. Liquid Biopsy

Liquid biopsy is a recent concept based on the analysis of tumour-associated components that circulate in the blood of cancer patients. Therefore, this biopsy basically consists in a blood sample collection that can be subsequently processed and analysed[44].

Several tumour-derived material can be isolated from this collected sample such as circulating tumour cells (CTCs), cell free nucleic acids and tumour-related extracellular vesicles, among others[45].

Another alternative source of tumour-related biological information that is the focus on several studies is tumour-educated blood platelets[46,47].

Moreover, the study of CTCs and ctDNA in the clinic has demonstrated to be useful for early diagnosis, accurate prognosis and personalised therapeutics. As such, liquid biopsy may overcome the limitations of current sampling methods in oncology since it is non-invasive and, therefore, can be easily repeated, obtaining information about tumour dynamics. Also, since cancer material is released in circulation from primary and metastatic lesions, liquid biopsy also provides information about tumour heterogeneity. Overall, and since CTCs and ctDNA have a short half-life in circulation, liquid biopsy can directly address clonal evolution of cancer, by obtaining real-time information about disease progression and resistance to treatment. In opposite, tissue biopsy is not only invasive, but sometimes it might not even be possible depending on the condition of the patient and the tumour location[48]. So, this methodology arises as a useful tool for monitoring the evolution of patients in real time, to predict cancer treatment responses, to evaluate treatment efficacy and for early detection of secondary mutations towards personalised therapy.

Although liquid biopsy has not yet fully entered clinical practice, it has a lot of potential to become clinical routine. In fact, in 2016, the first liquid biopsy test was approved by the FDA for the detection of EGFR mutation in non-small cell lung cancer, in which the analysis of cfDNA allows the selection of patients as responders for anti-EGFR therapy[49]. Research in the field works hence in this direction, to develop and transfer liquid biopsy technologies towards meaningful clinical applications in diagnosis,

monitoring, evaluating treatment response or resistance, and quantifying minimal residual disease, among others[48].

1.3.1. Liquid Biopsy in Colorectal Cancer

Currently, in CRC, clinical disease assessment and staging is based on histopathological tumour tissue analysis, however, it lacks in providing clinically useful prognostic and predictive information for each individual patient[50].

For this reason, there is an increasing interest in the use of liquid biopsy in the management of CRC patients. In fact, the presence of tumour material in the peripheral blood of patients has been identified as a potential biomarker with prognostic importance in different phases of CRC progression, not only in early diagnosis and identification of minimal residual disease, but also in the evaluation of response to treatment and clonal evolution of the disease[50,51].

Indeed, circulating tumour cells has been proven useful and with clinical implications either in early stage or metastatic cancer. Particularly in CRC, some studies have already demonstrated its prognostic value for cancer progression and survival, in addition to help the clinicians regarding therapeutic decisions since the presence of CTCs may represent an early indicator of disseminated disease[52,53].

The analysis of ctDNA has been reported as a promising tool in the clinical management of CRC since it allows the detection of tumour-specific mutations. Indeed, some studies reported a statistically significant correlation between disease stage and the presence of tumour associated genetic aberrations such as *TP53, KRAS* and *APC* in the blood of CRC patients, which could bring added value in the diagnosis of this pathology[54].

In regards with the detection of minimal residual disease in CRC after surgical procedure, a study conducted by *Tie et al*. suggested that ctDNA can persist in circulation after surgery, which can be associated with an increased risk of relapse in stage II colon cancer[55].

Still on this subject, current methods of residual disease monitoring and recurrence after post-treatment follow-up, are costly and frequently use radiological technologies, which have limited sensitivity for the detection of micro-metastases[56]. For that reason, methodologies based on liquid biopsy can emerge as an alternative monitoring technique since patients with residual disease can be identified through persistence of tumour-associated genetic aberrations.

Liquid biopsy is increasingly studied by the scientific community and for colorectal cancer several data show its potentiality in the management of CRC patients in different stages of disease, either using ctDNA or CTCs. But the use of this approach in the clinical practice is still far from happening, mostly because lack of standardization of the tests to be used[51].

1.3.2. Circulating Tumour Cells

During tumour development, cancer cells acquire various genetic and epigenetic alterations becoming a heterogeneous population of cancer cells. Some of these alteration events could result in cells with increased adaptations. The so-called circulating tumour cells, undergo epithelial-mesenchymal transition releasing themselves from the primary tumour, then penetrating into the bloodstream and relocating to a distant location, where they are able to adapt to the new environment and finally grow to form metastasis[57].

The presence of tumour cells in the blood was described for the first time by Ashworth, in 1869, in a metastatic cancer patient. Years later, in 1955, Engell observed that circulating tumour cells were present both in peripheral and venous blood and only after draining a tumour during an operation, he was able to observe a larger amount of tumour cells in the draining vein when compared to the peripheral blood[58]. But only in 1993, *Leather et al.* identified CTCs with conventional cytology and cytokeratin staining after isolating tumour cells from 42 colorectal cancer patients using a density gradient followed by cytospin and showed immune histological evidence of CTCs in 4 of these patients[59].

Even though epithelial cells die upon detachment and losing cellular assembly, through a process called anoikis, it is possible to observe carcinoma-derived cells in the blood (49)[60]. However, most of them die once in the bloodstream by suffering apoptosis either due to the action of the innate immune system, shear forces or even oxidative stress. So, it is thought that to resist death CTCs perform a diversity of mechanisms including taking advantage of blood platelets through direct interactions which end up forming an emboli that appears to be able to shield them from shear forces and avoid immune system detection[57,61].

Upon exit from the bloodstream, CTCs face new adversities because now they must undergo a mesenchymal-epithelial transition (MET) to be able to colonize and survive in the new tissue-specific microenvironment. This survival ability is thought to be driven partly by genetic programs present in the CTCs that are also likely to direct the

development of organ-specific metastatic spread[62]. The isolation and characterisation of these cells require methods of extreme sensitivity and specificity which usually tries to combine enrichment and detection methods.

Nowadays, CTC detection has been correlated with disease stage, relapse rate, and survival in different types of cancer, therefore holds the potential to, not only become an early non-invasive diagnosis of cancer, as well as a useful monitoring tool to predict and select the most appropriate treatment during the disease[63].

Although the major challenge to implement CTCs into the clinic continues to be the tumour heterogeneity that is reflected in the different populations of CTCs and their low number in circulation, these cells can still provide important genetic, phenotypic and functional information to understand cancer dynamics, to provide early and precise diagnosis and to select the most effective targeted therapy for each patient[57,64].

1.3.2.1. Circulating Tumour Cells in Colorectal Cancer

The detection and enumeration of CTCs as a tool in the clinical management of colorectal cancer has been proving very beneficial and, similarly to what happened with other epithelial malignancies, several studies showed that CTC counts have prognostic significance in the clinic. In fact, most studies demonstrated a clear association between worse prognosis and higher CTC counts[52].

The first studies performed on CTCs regarding colorectal cancer were conducted by *Cohen et al.* in 430 mCRC patients receiving chemotherapy. The results of the study suggested a high potential of CTC counts in the selection of patients who may sustain longer treatment breaks to minimise treatment toxicity without compromising treatment outcomes[52,65–67]. Curiously, the data obtained in this clinical trial supported the only US Food and Drug Administration (FDA) approved technology, the CellSearch® system, for enumeration of CTCs in metastatic colorectal cancer and is now commercially available[67].

Recent prospective studies demonstrated higher CTC concentrations in patients who had received previous chemotherapy, which could, on one hand, reflect a higher burden of the disease, but on the other hand could also reflect the accumulation of resistant cells in pre-treated tumours[68]. Indeed, there are growing evidences showing that more aggressive CTCs are responsible for multidrug resistance which allow these cells to avoid apoptosis and conventional therapy and consequently drive tumour growth[69].

These facts raise the question whether conventional anticancer therapies target the right cells. The truth is almost all conventional treatments do not have CTCs as therapeutic targets, but the cells from the primary tumour, which means they might be missing these circulating cells and therefore chemoresistant and radioresistant subpopulations as well[69].

Another prospective study in mCRC regarding CAIRO2 role in this malignancy explored the use of CTCs as a complementary predictive tool to current imaging modalities such as computed tomography (CT) imaging and the results suggested not only an increased accuracy for predicting tumour progression, but also allowed the patient classification as having either stable or progressive disease[70]. These type of correlation could also be achieved in other types of functional imaging, like positron emission tomography (PET) since targeted therapy can cause necrosis and tumour cavitation without shrinkage, which cannot be concluded by only analysing PET images[68].

A totally different scenario is presented regarding early CRC because the scarcity of CTCs indicates a far more limited prognostic value. CTCs have been mainly correlated to the metastatic development and are associated with advanced stages of disease, so it is much more frequent to detect these cells in metastatic patients rather than patients at an early stage. However, in some cases, it is possible to observe CTCs events in early stage patients, which is considered to be associated with poorer prognosis[68].

1.3.3. CTCs isolation: Available technologies

CTCs can be isolated through different technologies that are based on physical or biological properties of the CTCs. Physical properties comprise their size, density, electrical charge, or deformability, allowing the separation from blood cells without labelling. On the other hand, biological properties include capturing the cell by cell surface protein expression, either by using antibodies that recognise tumour associated antigens or common leukocyte antigens, which implies a positive or negative selection, respectively[71,72].

1.3.3.1. Isolation based on biological properties

The most common techniques for the isolation of CTCs lean on antibody-based methods. This type of methodology is possible because there are antigens on the surface of CTCs that distinguish cancer cells from blood cells, such as epithelial markers[73].

Until now, the CellSearch® system is the most widely used and the only method approved by the FDA for breast, colorectal and prostate cancer, operating through immunomagnetic antibodies conjugated against EpCAM, protein that is present in the surface of some CTCs, but not in blood cells. Then a cross characterization is performed by staining the captured cells to demonstrate the presence of the nucleus and by immunofluorescence analysis with antibodies against cytokeratin (CK) to demonstrate the epithelial origin of the cell, and CD45 to exclude leukocytes. So, in order to be considered a CTC a cell needs to be DAPI positive, Cytokeratin positive, but negative for CD45 (DAPI+, CK+, CD45-)[74].

Nonetheless, there are some limitations regarding the CellSearch system that are related to the expression of EpCAM for CTC detection since this protein is downregulated in many CTCs during EMT[74]. In addition, not all cancers have an epithelial origin and for those EpCAM will not be expressed, therefore other target antigens are needed to enrich the cancer cells, which means that in this system cell loss may be occurring during the CTC capture step[75].

But there are also other commercially available technologies such as AdnaTest designed by AdnaGen for the detection of CTCs in patients with prostate, breast, and colon cancers. Similarly, to CellSearch, this system is based on a magnetic isolation with an enrichment step of EpCAM-expressing cells, but here the detection is achieved by an RT-PCR assay that identifies putative tumour-associated transcripts[76]. However, it has the same limitation as CellSearch® since the cell enrichment is performed only through epithelial markers. In addition, in this technique there is not only the probability of obtaining false negatives due to the possibility of contamination, but after the identification of tumour cells, they are no longer viable[76].

1.3.3.2. Isolation based on physical properties

Several technologies have been developed to isolate CTCs relying on the fact that they are physically distinct from most normal blood cells. For example, CTCs (20-30 μm) an on average larger than blood cells (8-12 μm) and based on this, approaches like size-based membrane filters, size/deformation-based microfluidic chips, and size-based hydrodynamic methods are being proposed[77].

However, the simplicity of this kind of procedures as well as being label-free can also become a limitation, since the isolation might not be specific, negatively influencing their capture efficiency[77]. As a matter of fact, some morphological data regarding CTCs

have highlighted the heterogeneity present in these cells since they can either be round or oval shape and even their size can vary from 4 μm to 30 μm[78]. In addition, CTCs are deformable which could affect the isolation efficiency and loss of CTCs. Indeed, the selection of a specific capture size may yield reliable CTC isolation in most of the patient samples, yet inadequate performance across all patients[79,80].

CTCs can also be physically isolated considering their electrical charge. Assuming that cells are electrically neutral, yet polarisable in an electrical field, electric dipole moments are induced in cells which means that the magnitude and direction of these dipole moments mainly depend on the dielectric properties of each cell. So, the principle behind this type of CTC separation depends on the cell phenotype, physiological state and morphology, which is different in different types of cells[77].

Although these isolation physical-based methods have shown high recovery and purity rates, they are set aside mostly due to its sample processing methodology and extremely low processed volumes.

1.3.3.3. The role of microfluidics

Microfluidics implies the study of the behaviour of fluids in micro-channels, as well as the manufacturing of such systems. Microfluidic devices have a wide range of applications and have been used in various areas ranging from physics and chemistry to biology. Among their applications, microfluidics has been widely used in cancer research, and more specifically, in the capture and detection of CTCs[81].

This technology holds many advantages not only enabling a cost-effective, simple, and automated operation, as well as uses small quantities of samples and reagents to carry out highly sensitive detection. Additionally, it allows a one step process of sample loading, separation and capture of live rare cells that can be later analysed through cellular, microscopic or molecular techniques[79,81].

Like traditional technologies, in microfluidic devices the separation may also be based on the cell size or immune-capture, as these devices are designed and constructed with high control of their properties at the micrometre scale to allow an efficient cell separation[79].

CTC isolation based on antibodies can also be achieved with microfluidic devices in which its large surface area is coated with ligands or capture molecules, that bind to CTCs due to the antigens present in its surface, like EpCAM. Therefore, when CTCs flow across the device, the tumour cells will be retained[79,82] . But for this method to be efficient

requires optimization of antibody immobilization processes to facilitate strong interactions between cells and the surface-bound capture molecules.

Many microfluidic systems for CTC isolation based on size have been developed such as Parsortix System, a size and compressibility-based platform for CTCs isolation, allowing capture of viable cells with high efficiency. However, this methodology as many other size-based technologies have the difficulty to completely separate cancer cells and leukocytes by their size[83]. Another size-based technology widely used is Vortex, which allows CTC isolated in less than 1 h, with high purity and good cumulative efficiency[84]. Furthermore, this approach opens up possibilities for the capture CTC characterization, to obtain information on proliferative and invasive properties or, ultimately, tumour re-initiating potential and response to drug[84].

Many microfluidic devices with promising results are under development. Some of them have already begun to enter in a variety of clinical trials. Nevertheless, their clinical application remains challenging because of the high quality standards needed to obtain certification, including system reliability, performance and minimal inter-user or inter-laboratory variability[81].

The RUBYchip™ is a microfluidic device fully designed, developed, and manufactured by the Medical Devices group at the International Iberian Nanotechnology Laboratory (INL) with the main purpose to capture viable CTCs according two different characteristics, the cell size and deformability.

Design wise the device is organized in two principal areas, each one containing four separated modules and in each module is possible to observe a single row of micropillars, distanced from each other in 5 μm, forming the filtering area in which potential CTCs will be retained, as illustrated in figure 3. Previous studies using earlier generations of this device have shown the capacity to process 7,5 mL of whole blood with no need of pre-processing.

The microfluidic masters were designed in 2D AutoCAD software and fabricated on a 200 mm silicon wafer using photolithography and deep reactive ion etching as described on *Ribeiro-Samy et al.* [85].

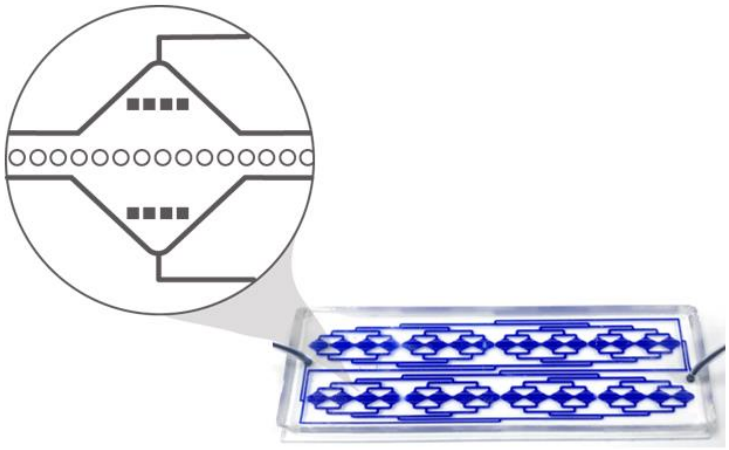

Figure 3 The RUBYchip™ design to capture CTCs based on physical properties such as size and cellular deformability. Focusing on the filtering area, which is composed by micropillars, distanced from each other in 5 μm.

Prior to the RUBYchip® development, other microfluidic-based platforms aiming the isolation of CTCs with high efficiency and without the need of blood sample pre-processing were achieved by Medical Devices group at INL. While the first generation of these devices, called Mini, was only able to process 1 mL of whole blood samples, further developments resulted in a second generation of these devices, the Cross, which was able to process 4 mL of whole blood samples. Later, a third generation was achieved, the Mega, in which 7.5 mL whole blood samples could be processed. Finally, Mega redesign to half its size led to the development of the RUBYchip®, with the same processing capacity, however able to fit in standard microscope glass side.

In the last years, several studies have been conducted using whole blood samples from metastatic colorectal and bladder cancer patients in order to validate the microfluidic device[85–87]. In these studies, high isolation efficiencies were reported, in addition to discriminate patients with good prognosis from those facing an unfavourable outcome[85].

2. Objectives

Every individual is different, and so is every patient. Recognising that each patient needs an appropriate follow-up to its own illness will allow for a more accurate treatment with fewer side effects which ultimately will provide a better quality of life and longer survival rates. So, the research for a non-invasive approach for precise diagnosis that is sensitive and specific for each patient has been a continuous challenge for the scientific community. There is a growing demand in implementing liquid biopsy in the clinic such as the capture of CTCs to be applied whether in diagnosis, to complement tissue biopsy, or in screening and prognosis of cancer patients, especially in colorectal cancer.

In this context, this master thesis aims to optimise a microfluidic device, the RUBYchip™, for the isolation and characterisation of CTCs from the blood of colorectal cancer patients. Hence, it comprises the evaluation of the device efficiency to get the optimal sample processing parameters using colorectal cancer cell lines. It is also envisioned the assessment of vimentin expression in CTCs to further understand the epithelial versus mesenchymal type of CTCs and its meaning in CRC patients.

Thus, this work aims to accomplish the following specific objectives:

- Flow rate determination and capture efficiency assessment of the RUBYchip™ using colorectal cancer cell lines.
- Optimization of the immunostaining protocol to be applied as the criteria set in the colorectal cancer patient samples.
- Optimal parameters validation in whole blood samples from patients with metastatic colorectal cancer.

3. Materials and Methods

3.1. Device fabrication

For the fabrication of the microfluidic devices, 9 masters were available to rapidly obtain replicas through a technique named soft lithography. First, a polymer was prepared by mixing polydimethylsiloxane prepolymer with a cross-linker (PDMS, SYLGARD™ 184 Silicone Elastomer, Dow Chemical Company) in a ratio of 10:1, followed by degassing in the desiccator to be then poured over the master, degassed again and cured at 65°C for at least a minimum of 2 hours or left overnight to solidify.

After cured, the PDMS was peeled off from the master with the help of a scalpel and then both inlet and outlets were punched using a 1.25 mm biopsy puncher (World Precision Instruments). Finally, to obtain the device, both the PDMS replicas and glass slides (size 25x75 mm, ThermoFisher Scrientific), previously cleaned with Hellmanex (Hellmanex III, Hellma Analytics), were treated with oxygen plasma at medium power for 30 seconds to be then brought in contact to produce irreversible bonding.

In the end, 30 cm ethyl vinyl acetate microtube (51x 0.5mm ID x 1,5mm OD EVA, ColeParmer) was inserted both in inlet and outlet of the microfluidic device and in order to connect the inlet to a syringe a blunt needle (LS22K Luer Stub, Instech) was used.

To finalise device fabrication, functionalization of the devices was required to avoid unspecific attachment of cells onto the channel surface. Hence, using a syringe pump (NE-1200, New Era Syringe Pumps) three solutions were injected into the device.

Right before the functionalization process, the devices were subjected to an inspection test under the inverted Nikon MA200 microscope to check on the bonding and to verify whether the filtration areas were clear and fibre-free as the device manufacturing procedure is not carried out under strict aseptic conditions.

Then to prime the microchannels the functionalization process was conducted. First, to enhance wettability 350 µL of ethanol (Sigma Aldrich) were pumped at 100 µL/min, followed by 350 µL of 10 mM Phosphate Buffer Saline (PBS, Sigma Aldrich) at 120 µL/min, as a washing step. Finally, 4000 µl of the same solution were injected in the chip in order to stress test the device with a volume of the same magnitude as the blood sample that will be processed, thus assuring an efficient performance during blood sample processing. The protocol explained above is illustrated in figure 4.

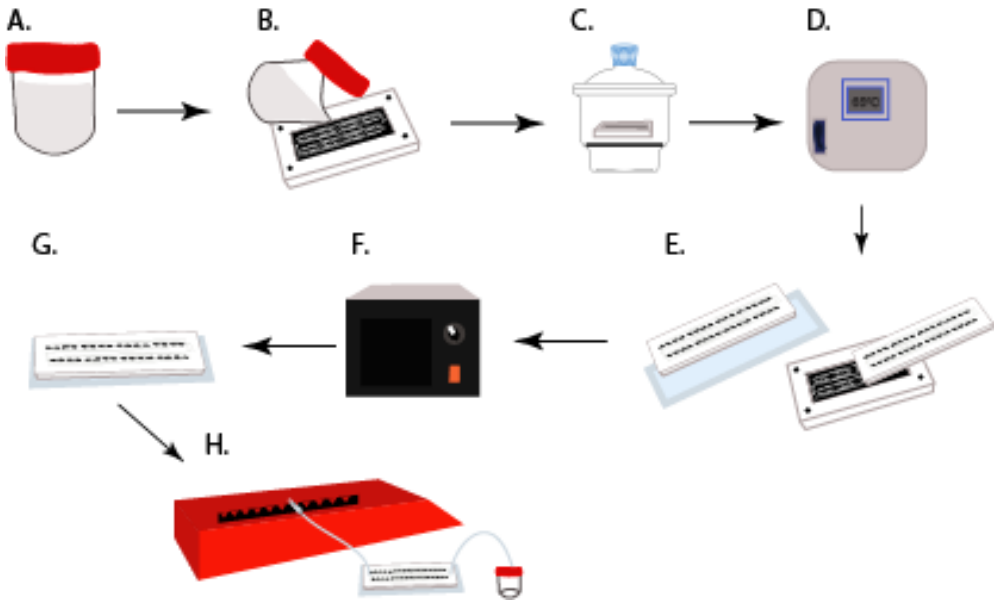

Figure 4 *Device Fabrication. (A) PDMS polymer is prepared by adding PDMS elastomer and crosslinker in a 10:1 ratio and vigorously mixed, afterwards the aerated mixture is degasses using vacuum. (B) Once degassed the PDMS is poured over the master. (C) The master is also put under vacuum to further degas the PDMS. (D) The master is brought to the oven, at 65ºC for 3h to cure the PDMS. (E) Once the PDMS is cured, the replica is peeled off from the master, and inlet and outlet holes are punched. (F) Previously cleaned and inspected replica and glass slide are put under oxygen plasma treatment, to allow irreversible linkage between them. (G) The bonding between the replica and the microscope glass is performed. (H) The device is connected to a syringe pump to proceed with device functionalization.*

The device fabrication was included in the weekly tasks, 2 to 3 days, in order to guarantee a reasonable stock for experimental needs. At the lab scale, even though a large number of devices are achieved, device fabrication efficiency is not 100%, which means that is expectable to have losses during this process.

After assembled, each device was nominated according with the master number from which the replica was achieved, the number of replica from that specific master and the total number of fabricated devices. This information was registered in the course of this year in a logbook as schematized in figure 5.

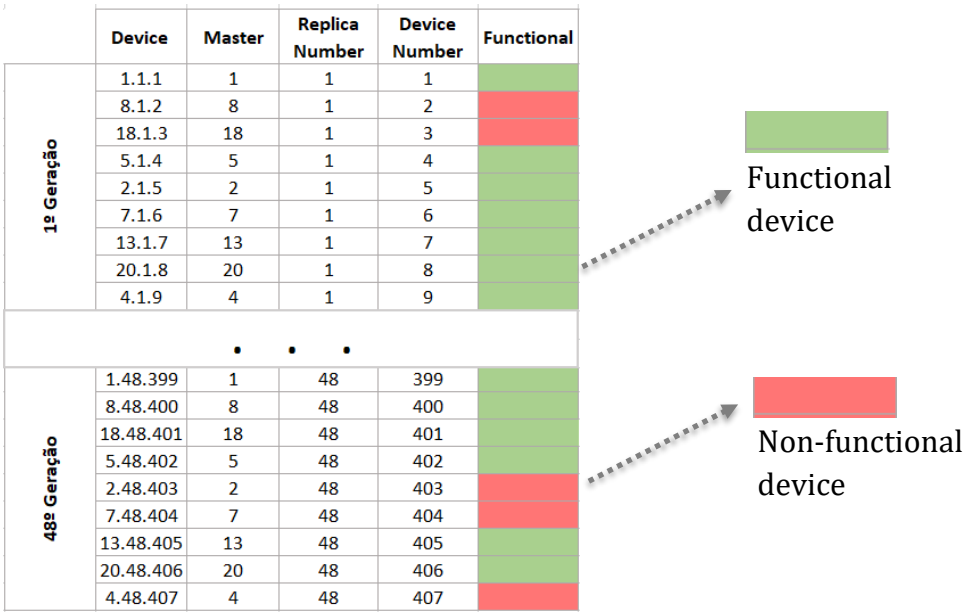

Figure 5 *Schematic representation of the device fabrication logbook to keep track of the functional and non-functional fabricated devices.*

3.2. Cell culture

For cell culture and cell experiments, four colorectal cancer cell lines were used namely SW480 (ATCC, CCL-228), Caco-2 (ATCC, HTB-37), RKO (ATCC, CRL-2577) and HT-29 (ATCC, HTB-38), all of them kindly provided by medical devices group at INL.

All CRC cell lines were cultured in Dulbecco´s modified eagle medium (DMEM) supplemented with 1% Penicillin/Streptomycin (PS) and 10% fetal bovine serum (FBS) except for Caco-2, which required a 20% FBS supplementation. Cultures were kept in an incubator at 37°C and with 5% CO_2 humidified atmosphere.

3.2.1. CRC cell lines thawing

All the cell lines were thawed following the same protocol, except RKO that were kindly provided by colleagues already in culture. Firstly, they were removed from the -80ºC freezer and rapidly defrost in a 37˚C water bath. When thawed, the vial was removed from the bath and decontaminated by spraying with 70% ethanol and all the subsequent operations were carried out under strict aseptic conditions. Next, the vial content was transferred to a falcon containing complete culture medium, and spin at approximately 225xg for 5 minutes.

The resulted cell pellet was resuspended with the recommended complete medium for each cell line and dispense into a new culture T25 flask, that was then kept in an incubator at 37˚C with 5% CO_2 humidified atmosphere.

At each starting culture, cells were closely monitored by observation and imaging under the microscope for 72 h, or until the regular growth pace was achieved, as schematized in figure 6.

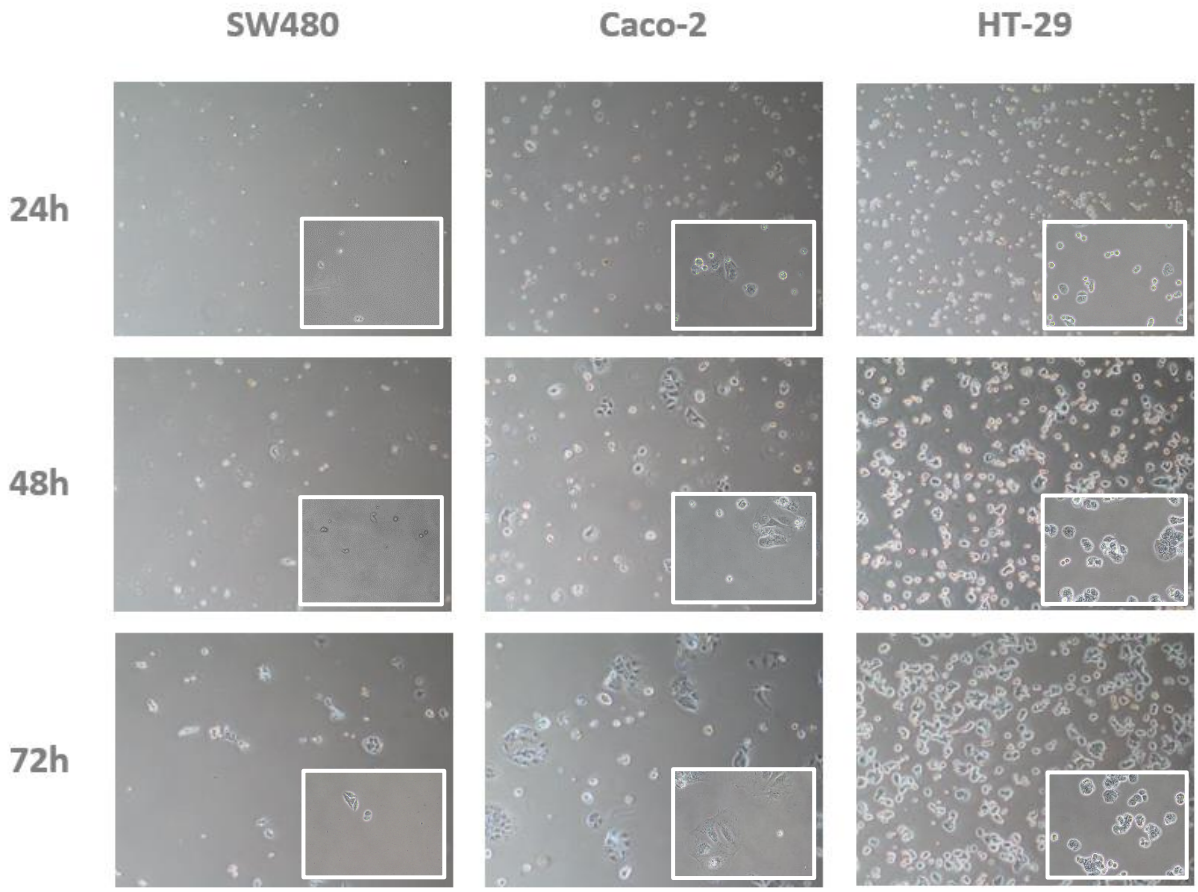

Figure 6 *SW480, Caco-2 and HT-29 cells were closely monitored. Cell confluence images at 24, 48 and 72 hours after starting the cell culture. Images were obtained in inverted microscope with x4 objective and analyse through NIS software.*

3.2.2. CRC cell lines freezing

Once the cells were in culture, growing at the normal pace, a cell freezing protocol was conducted in order to store them for future needs. At full confluence, cells were briefly rinsed with 0.25% (w/v) Trypsin-EDTA solution and then placed at 37˚C to facilitate dispersal. Trypsin was then neutralised with fresh medium. After which the solution was transferred to a sterile centrifuge tube, to be centrifuge at 225xg for 3-5 minutes.

In the end, the resultant pellet was quickly re-suspended in freezing media composed by each cell line specific media with 5% DMSO to be subsequently distributed in cryovials to be frozen and stored in liquid nitrogen.

3.2.3. CRC cell culture maintenance

The cells were routinely maintained with medium renewal every 2 to 3 days and sub-cultured when reaching about 80-90% confluency. In figure 7, is possible to observe 95-100% confluent cells in each cell line.

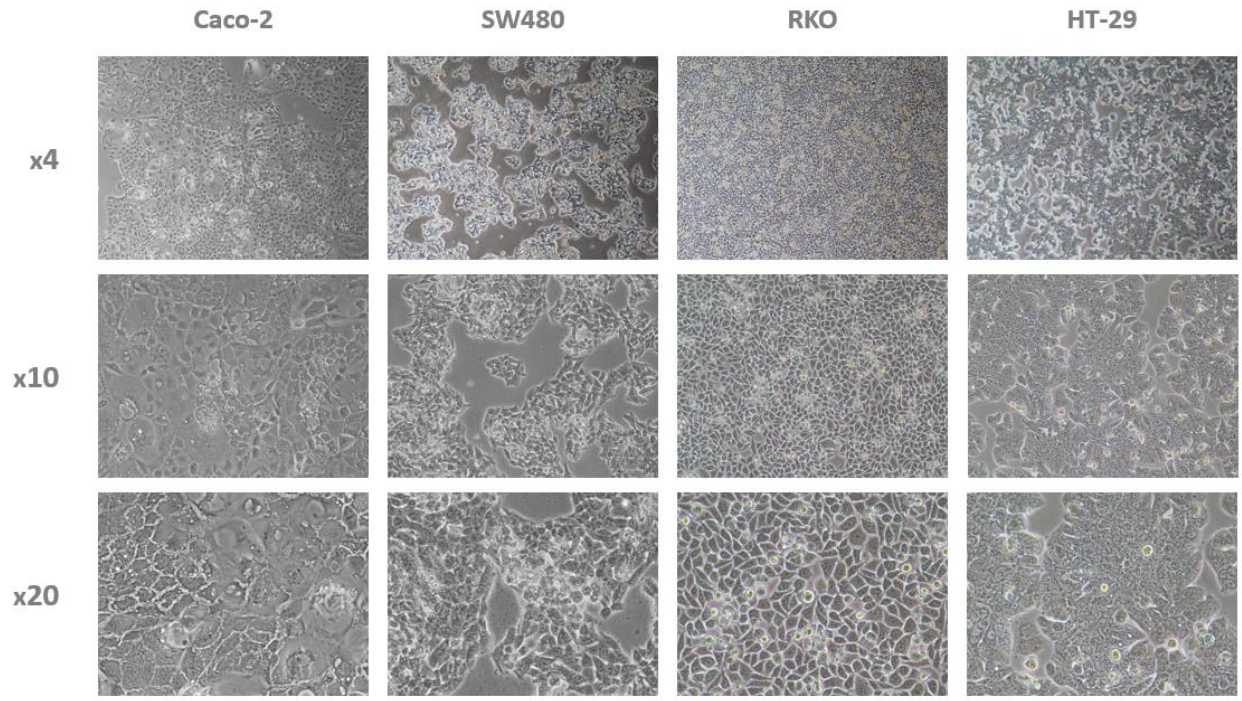

Figure 7 *Acquired images from colorectal cancer cell lines (Caco-2, SW480, RKO and HT-29) at high confluency and monolayer.*

At this confluence, growth medium was removed and discarded, followed by the addition of PBS, as a washing step to remove any serum detritus that could inhibit trypsin action. Then, the cell layer was rinsed following the standard protocol explained above. Subsequently, the trypsin was neutralized by adding complete growth medium to the cell suspension. After gently resuspended, viable cells were counted in the Neubauer Haematocytometer (Hirschmann® EM Techcolor) by adding 10 µL of a solution containing Trypan Blue (Corning) and 10 µL of the cell suspension, after which was taken to an inverted microscope for cell counting.

Of note, only viable cells were counted to then calculate the cell density through equation 1. Finally, cells were transferred to a new T25 flask in the recommended subcultivation ratio.

Equação 1: $Cell\ Concentration = \frac{Total\ Cells\ Counted}{4} \times 10^{-4}$

3.3. Spiking experiments

3.3.1. Flow rate influence

In order to determine the optimal parameters for the processing of blood samples from colorectal cancer patients, several spiking experiments were performed. For this purpose, the four cell lines previously mentioned were used since they have morphological differences such as size and deformability.

At approximately 90% confluence, adherent cells were harvested by incubation in 0.25% Trypsin-EDTA to obtain a cell suspension, which was then transferred to a falcon tube. Cell density was obtained using the haemocytometer according to the protocol described above. After estimating cell density, $6{,}0 \times 10^5$ cells were transferred to a new falcon tube and the appropriate volume to achieve a total volume of 2 ml was added. To stain the cells, the solution was then centrifuged at 225xg for 5 minutes at room temperature (RT) and the resultant pellet was brought to suspension and incubated with Hoechst (Invitrogen®, ThermoFisher Scientific) for 30 minutes. Then, as washing steps, several centrifugations were performed at 225xg for 5 minutes each.

After which an additional cell counting was performed using the Neubauer haemocytometer, following the standard protocol, to assess the cell number in the stock cell suspension after which step-by-step serial dilutions were prepared, as detailed in figure 8, to obtain a final cell suspension of 1000 cells / 1mL (200 cells per 200µl).

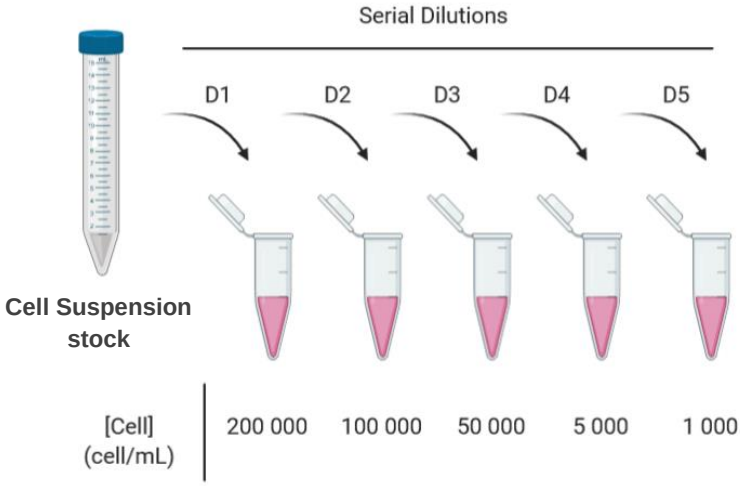

Figure 8 *Schematic representation of the serial dilutions performed in spiking experiments in order to obtain final a cell concentration of 1000 cells/mL.*

In order to determine the optimal capture efficiency of the microfluidic device, five different flow rates were tested, namely 80, 100, 120, 160 and 200 µL/minute in experiments performed in triplicate. Thus, 200 cells were spiked in 7,5 mL of whole blood samples collected from healthy donors and injected into the device using a syringe pump. Afterwards, to wash 350 µL of 2% Bovine Serum Albumin (BSA, Sigma Aldrich) were injected in the device, followed by 350 µL of 4% Paraformaldehyde (PFA, Sigma Aldrich) incubated for 20 minutes to fix the cells. Lastly, as a second washing step, 350 µL of 0.01M PBS was pumped through the device.

Once these steps were concluded, the device was taken to the fluorescence inverted Nikon TI-E microscope to perform the manually counting of the Hoechst positive trapped cells. This value was then compared to the total number of spiked cells to obtain the capture efficiency of the RUBYchip™, as in the following equation (equation 2).

Equation 2: $$CTC\ Capture\ efficiency\ (\%) = \frac{Trapped\ CTCs}{Spiked\ Cells} \times 100$$

3.3.2. Cell target influence

The protocol previously described was performed to evaluate the influence of different cell target numbers, number of cell spiked into the blood sample, in the capture efficiency. Thus, 50, 200 and 1000 cells of the different CRC cell lines (SW480, Caco-2 and HT-29) previously stained were added to 7,5 mL of whole blood samples collected from healthy volunteers and then processed in the device at the optimal flow rate earlier determined.

In the end, the devices were taken to the fluorescence inverted microscope to proceed with the cell counting, which was then compared to the total number of spiked cells in order to determine the capture efficiency.

3.3.3. Cell size and nucleus-to-cytoplasmatic ratio

Cell dimensions, namely cell size and nucleus size, were assessed using NIS-Elements analysis software from Nikon, in acquired images obtained from spiking experiments. In detail, using a tool that allows measuring the distance between two points, it is possible draw the cell diameter (spherical diameter) in the selected cell event and determine cell size in micrometres. Only individualized and bright field clear cell events were used, cell limits were confirmed adjusting the contrast of the bright field. Cell nucleus size is determined in a similar way, measuring nuclear diameter using the same NIS tool, its circular limits can be clearly observed since cells are stained with Hoechst nuclear dye, as showed in figure 9. Then, to achieve the nucleus-to-cytoplasm (N:C) ratio the following equation was used (equation 3).

Equação 3: $NC\ ratio = \frac{Nucleus\ size}{Cell\ Size}$

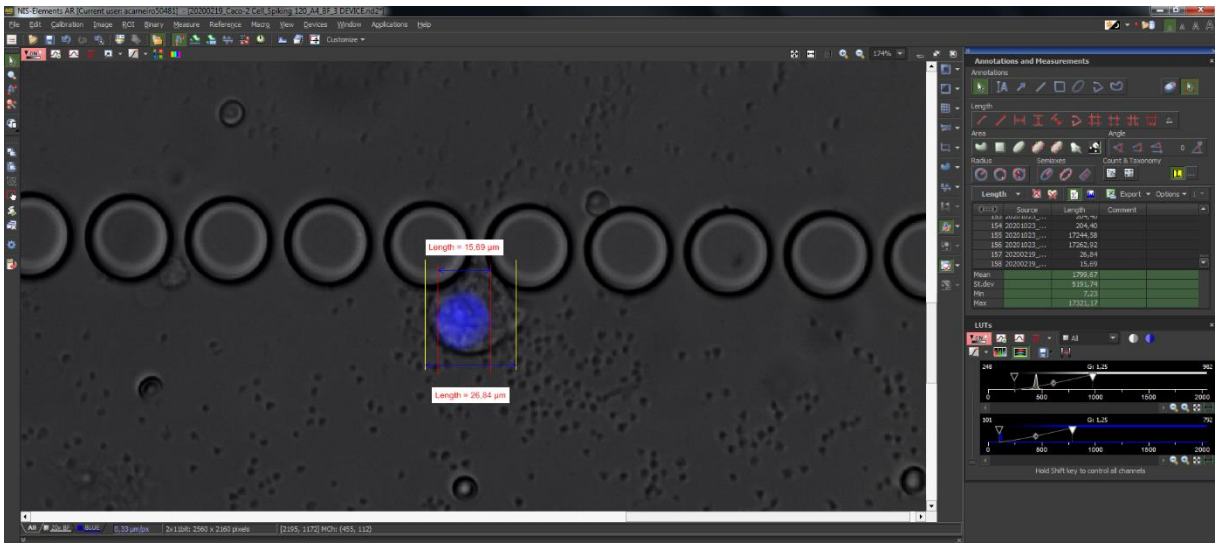

Figure 9 *Schematic representation of NIS- elements analysis software namely the cell measuring used tool*

3.4. Immunocytochemistry studies

In this study, CTC identification was achieved by antibody (Ab)-based methods. Therefore immunocytochemistry (ICC) assays were performed to select and optimise the antibody panel to be used in the analysis of clinical samples.

All antibodies chosen were purchased already conjugated with fluorophores which allows to perform direct immunofluorescence. In this way, the protocol is performed faster, and risk of cross-reactivity is minimised when using antibodies combined in a cocktail solution.

Thus, an anti-Pan Cytokeratin was used to positively select epithelial cells, an anti-vimentin antibody to identify mesenchymal events and, finally, an anti-CD45 antibody as an exclusion criteria of CTCs, since it allows to identify white blood cells (WBC). In addition, DAPI (NucBlue™; Invitrogen) was used to stain the cell nucleus. All the tested antibodies are detailed in table 2.

For this study, each fluorochrome was chosen in accordance with the emission and excitation filters of the fluorescence inverted Nikon- TI-E microscope, which is used for image acquisition.

Table 2 *Tested antibodies specifications*

Target Protein	Antibody	Biological Source	Conjugate Fluorophore	Emission // Excitation (nm)	Company
Cytokeratin	Monoclonal Anti-Pan Cytokeratin	Mouse	FITC	530//365	Sigma Aldrich
		Mouse	Alexa Fluor 488	525//490	ExBio
Vimentin	Monoclonal Anti-Vimentin	Mouse	eFluor 570	570//555	Invitrogen by Thermo Fisher Scientific
CD45	Polyclonal Anti-Human CD45	Rabbit	Cy5	670//625	Immunostep®
	Monoclonal Anti-Human CD45	Mouse	Alexa Fluor 647	665//650	Santa Cruz Biotechnology

3.4.1. Immunocytochemistry studies performed in well-plate

Firstly, ICC experiments were performed in well plate using the CRC cancer cell lines previously mentioned (SW480, HT-29 and Caco-2), as well as peripheral blood mononuclear cells (PBMCs) isolated from blood of healthy volunteers.

To conduct these experiments cell lines were seeded in 24-well-plates, on sterile cover slips (13 mm in diameter) previously treated with Poly-Lysine (Sigma) to promote cell attachment to the glass surface. Prior to cell seeding, a brief set of experiments were carried out to assess which was the ideal cell seeding for each cell line to grow up to 72h, until ICC was performed (results not shown). Ideal cell seeding for SW480 and HT-29 was found to be $45x10^5$ cells per well and for Caco-2 is $35x10^5$ cells per well. As mentioned, cells were left to grow for 72h and later stained with different antibodies dilutions.

PBMCs were isolated from blood of healthy donors through density gradient centrifugation using Histopaque® (Sigma Aldrich). The whole blood sample was transferred to a falcon tube and diluted in 2% PBS/FBS on a 1:1 volume ratio. In a new falcon tube, containing the Histopaque® in a 2:1 dilution, the diluted blood was carefully poured followed by a centrifugation for 30 minutes at 400xg. Differential migration during centrifugation results in the formation of layers containing the different blood components. It is possible to observe in the falcon tube, a top layer composed by plasma, which was removed and discarded. In the following layer, the mononuclear cells were gently harvested and subsequently washed with the appropriate buffer, 2%PBS-FBS,

through serial centrifugations for 10 minutes at 300xg as detailed in figure 10. Bottom layer contains mainly erythrocytes that have aggregated, as shown in figure 10.

To proceed to count the mononuclear cells, a Neubauer haemocytometer was used as previously explained and, $2x10^6$ of PBMCs were used for each tested condition. Of note ICC protocol of PBMCs, as non-adherent cells, was performed in Eppendorf tubes.

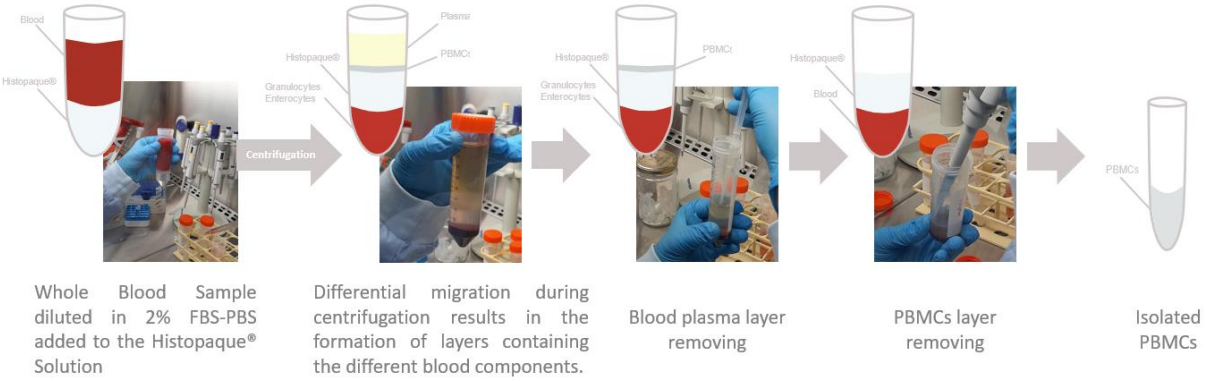

Figure 10 *Schematic representation of the PBMCs isolation protocol.*

To proceed with the ICC assay, both adherent cells and isolated PBMCs were fixed with 4% PFA and incubated for 20 minutes. After a washing step with 500 µL PBS (0.01M, pH 7.4), cell permeabilization was achieved by adding 0.25% Triton X-100 (Sigma Aldrich) in (prepared in 0.01M PBS), incubated for 10 minutes, except when CD45 would be added.

A new washing step with 500 µL PBS was performed and then, to prevent unspecific bindings, blocking was performed in 500 µL of 2% BSA (prepared in 0.01M PBS) and incubated for 30 minutes, followed by a last washing step with 500 µL PBS.

Finally, the cells were incubated with 120 µL of the antibodies, at the dilution to be tested, at room temperature for one hour and fifteen minutes in dark. After antibody incubation, two washing step were done, first with 0.5% BSA (prepared in 0.01M PBS) and finally with PBS.

The ICC protocol was run in parallel for adherent cells in 24-well plates and for PBMCs in eppendorf tubes.

Experimental design is schematized in figure 11.

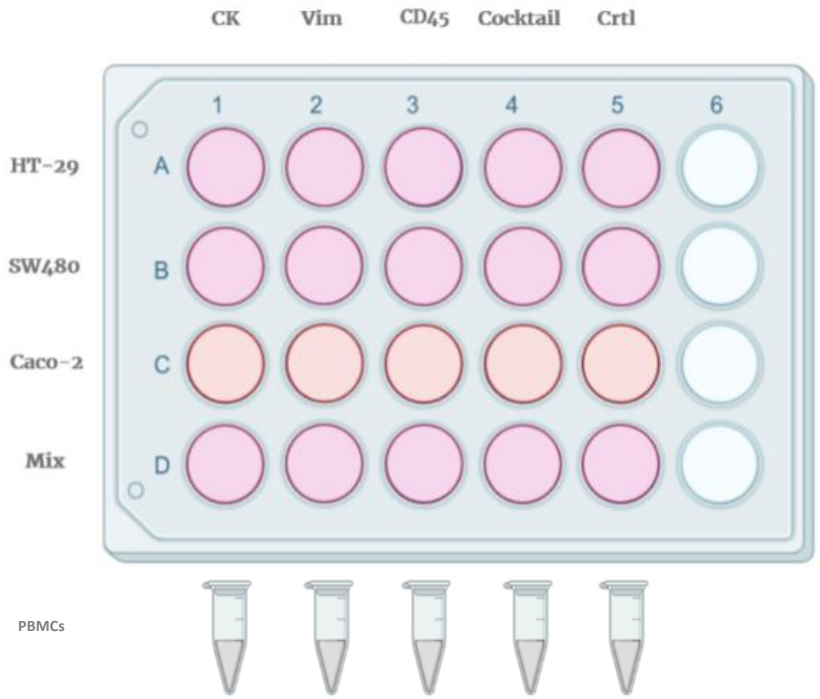

Figure 11 *Experimental design of Immunocytochemistry performed on well-plate in CRC cell lines and isolated PBMCs.*

Afterwards, in order to observe the cells under the fluorescence microscope, the coverslips with the adherent cells and PBMCs were mounted with the cells facing towards a microscope slide on a drop of Mounting Medium (Anti-Fade Fluorescence mounting Medium- Aqueous, Fluoroshield, Abcam). Coverslips were immobilized on a glass slide.

In order to be able to stain cultured cells combined with PBMCs in a single condition, adherent cells were brought into suspension and both cell types were mixed, to carry out the protocol.

To accomplish this, the cells were distributed into a 48-well plate at the following densities, $1x10^5$ of HT-29 and SW480 cells, $5x10^4$ of Caco-2 cells and $5.0x10^6$ of PBMCs in each condition, as schematized in figure 12.

Step-by-step immunofluorescence was carried out as described above, except in this case high speed centrifugations were used, since cell mixtures were used in suspension in well plate.

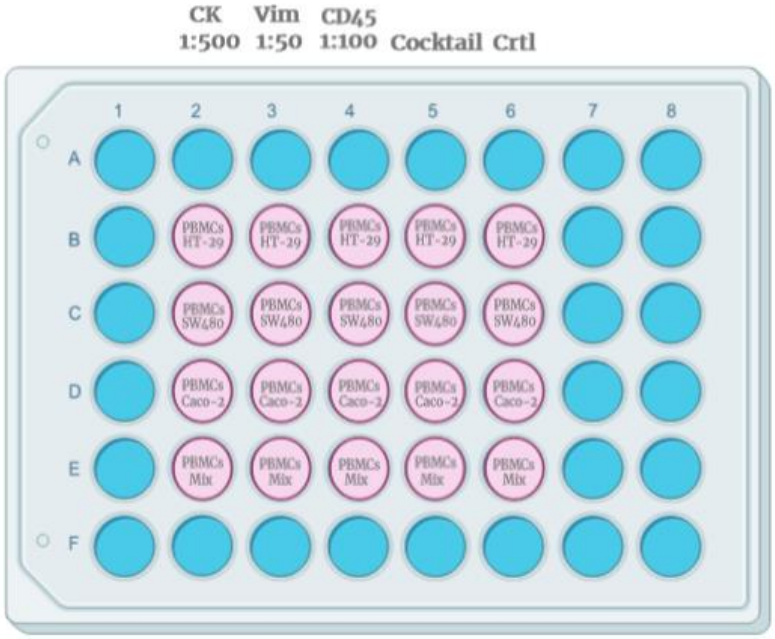

Figure 12 *Schematic representation of the ICC experiment performed in well plate to test the antibody panel (CK 1:500, VIM 1:50, CD45 1:100). Here the PBMCs were mixed with the cells in all the tested conditions.*

3.4.2. Immunocytochemistry studies performed in-device

Afterwards, in order to test the antibody panel on the RUBYchip™ and mimic the processing conditions of cancer patient samples, several ICC experiments were performed.

Same step-by-step ICC protocol was strictly performed as described previously, however in order to fix, permeabilize, block, stain and wash cells trapped inside the microfluidics device all reagent solutions were pumped into the device at predetermined flow rate using a syringe pump.

To begin with, negative controls were performed using the selected antibody panel to stain samples from healthy donors alone. Simultaneously, two different approaches to the ICC protocol were tested to assess which methodology would be best to be use in future experiments:(I) all antibodies in a single-step using a cocktail and about 1hour incubation; and (II) a step-by-step protocol, in which each antibody was sequentially incubated for about 1hour, at room temperature.

Negative controls (samples without cultured cells spiked), either healthy donor's whole blood samples or isolated fraction of PBMCs were further used to test either complete cocktail, cocktail without CK antibody or CK antibody alone.

Lastly, in order to closer mimic CTCs circulating in blood, cocktail solutions of antibodies were tested into spiked samples, SW480 cultured cells were spiked either in healthy donor whole blood samples or isolated PBMCs fraction also from healthy donors. Experimental design is schematized in the figure below (figure 13).

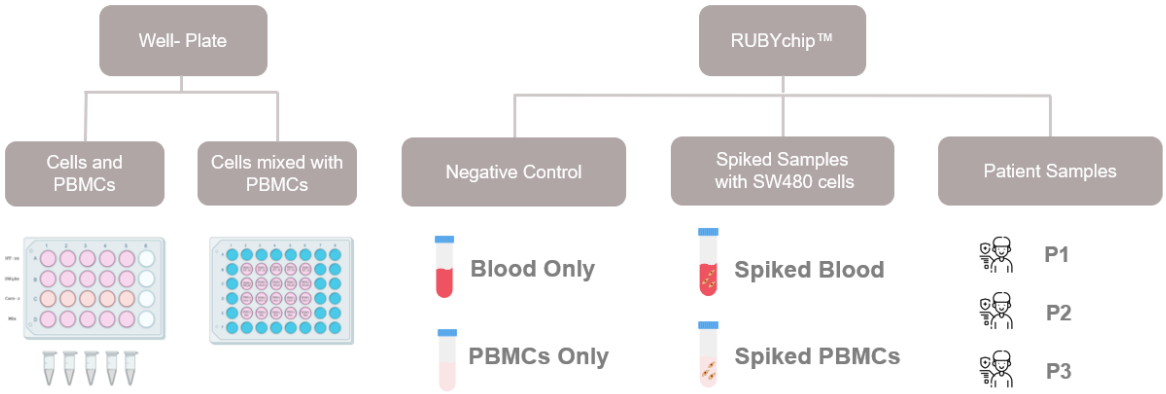

Figure 13 *Schematic representation of the ICC experimental design in all cell lines in plate and, in processed samples in the device*

Finally, all microfluidic devices were visualized in Nikon Ti-E microscope and later analysed with NIS® software from Nikon. For cell analysis, isolation areas of the microfluidic device are imaged and a total of 8 large scans are obtained per device. Each image includes 22 fields of view, covering for an approximate device area of 1.8x0.07 cm. Each image scan is obtained by simultaneously acquisition of 4 fluorescent channels (Blue, Green, Orange and Red), plus Bright Field.

3.4.3. Immunocytochemistry studies in clinical samples

3.4.3.1. Patient sample collection

For a small proof-of-concept, 3 metastatic colorectal cancer patients diagnosed at Instituto Português de Oncologia (IPO) in Porto were recruited according to the following condition: patients must be recently diagnosed with colorectal cancer, already presenting metastatic lesion at the moment of the diagnosis. Blood collection was performed before any cancer treatment. After approval of the study by the ethics committee of the hospital, all patients enrolled voluntarily and signed an informed consent to participate in the present study.

A total of 7.5mL of peripheral blood was collected from each patient in an EDTA-coated tube. Tubes were immediately shipped to INL in Braga to be processed within four to six hours and analysed afterwards.

3.4.3.2. Patient sample staining and analysis

To validate previous findings, CRC patient samples were stained for CTC analysis, using antibody panel and conditions described previously. Patients whole blood samples were processed at the optimal flow rate previously determined, stained with antibodies, and imaged at the Nikon Ti-E microscope, according to the protocol described above. In table 3 is summarized the operation program of size-based microfluidic device for the processing, staining and analysis of the captured cells.

For further image analysis, a set of criteria according to standard CK and CD45 immunostaining and morphological features was established to classify trapped cells.

Briefly, CTCs were defined as nucleated, determined by DAPI staining, and expressing either CK and/or VIM and lacking the marker of hematopoietic lineage CD45 ($CK^+/CD45^-$ or $VIM^+/CD45^-$). In this study, epithelial and mesenchymal biomarkers present green and orange fluorescence, respectively and CD45 present red fluorescence.

In addition, CTCs were also characterized morphologically by a large nucleus and large NC ratio, defined in this study as the imaged area of the nucleus to the area of the surrounding cytoplasm.

Table 3 *Operation program of size-based microfluidic device for whole blood processing, staining and analysis of the trapped cells.*

Operation	State	Volume (µL)	Time (min)
1. Blood Processing	Flow	7500	75
2. Washing	Flow	350	3,5
3. Cell Fixation	Incubation		20
4. Washing	Flow		3,5
5. Permeabilization	Incubation		10
6. Washing	Flow		3,5
7. Blocking	Incubation		30
8. Staining	Incubation	250	75
9. Washing	Flow	350	3,5
10. Image Acquisition	Microscope		120
11. Image Analysis	NIS Software		180

Cells population were analysed and counted manually in a scanning area of 200µm above and below post line, using NIS® software from Nikon according to the criteria schematized in figure 14.

Classification	DAPI	CK	VIM	CD45
Epithelial CTCs	+	+	-	-
EMT CTCs	+	+	+	-
Mesenchymal CTCs	+	-	+	-
White Blood cells	+	-	+/-	+
Double Staining	+	+	+/-	+

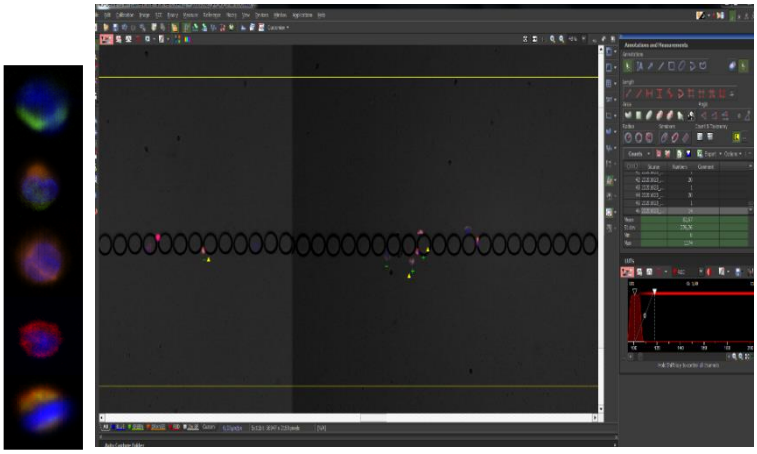

Figure 14 *Immunofluorescent staining characteristics for identifying CTCs*

3.5. Statistical analysis

A non-parametric t-test was used to compare the different cell targets (50 *vs* 200; 50 *vs* 1000; 200 *vs* 1000) in each cell line.

Statistical analysis was conducted using GraphPad Prism Software (Graphpad Software, version 8.0.1, San Diego, CA®). A p value lower than 0.05 was assumed to denote a significant difference.

4. Results and Discussion

4.1. RUBYchip™ performance assessment using human CRC cell lines

The RUBYchip™ was designed to capture cancer cells through two main characteristics, their size and cellular deformability. Indeed, the geometry of the RUBYchip™, in addition to its surface treatment, creates a favourable environment for CTC entrapment. The device dimensions are ideal to allow smaller or larger, but deformable cells, like blood cells, to pass easily through the filter gaps. Simultaneously larger cells, but less deformable due to the smaller nucleus-to-cytoplasm ratio, like cancer cells, will likely be retained. Spiking experiments aim to mimic patient sample conditions, so as mentioned, in these experiments cultured cancer cell lines are introduced into healthy donor whole blood samples to evaluate RUBYchip™ capture efficiencies.

4.1.1. CRC cells dimension assessment

It was relevant to assess cell dimensions of the tested CRC cell lines inside the device since they are in suspension and circularized instead of adherent, and since this aspect will heavily influence their chance to be captured by our device.

In all cell lines, it was possible to observe size variation, which could be related to the different cell stages of the cell cycle. For that reason, it was determined a size range for each cell line as following Caco-2 (14.94-35.17 µm); SW480 (12.24-24.39 µm), HT-29 (8.75-22.68 µm) and finally, RKO (8.18-16.91 µm), as illustrated in figure 15.

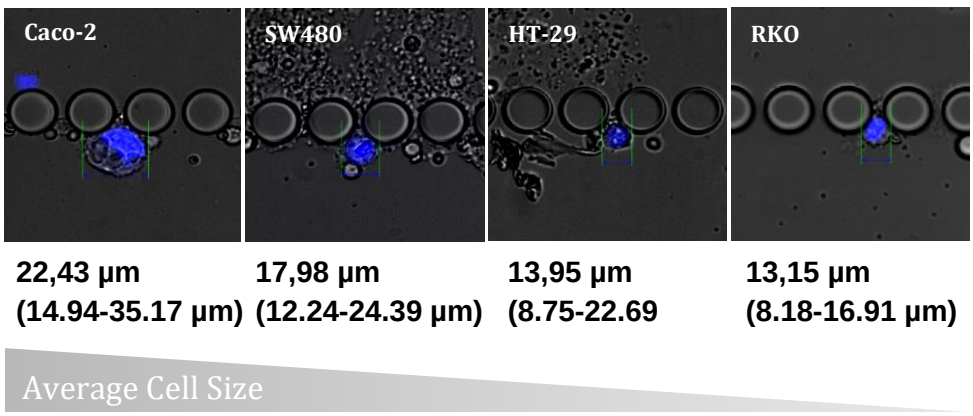

Figure 15 Schematic representation of the cell size on average, as well as the size range for each cell line. Cell nucleus was stained with Hoechst.

Indeed, the largest cells were Caco-2 with an average size of 22.43 µm, followed by SW480 with 17.98 µm, lastly the smallest and very close in size are HT-29 with 13.95 µm and RKO cells with 13.15 µm, as represented in figure 16.

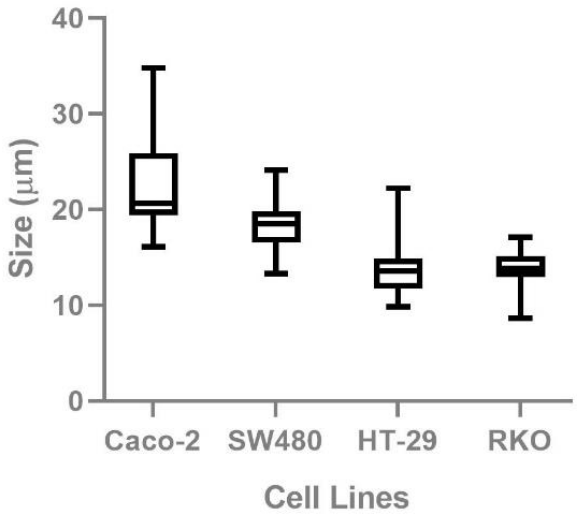

Figure 16 *Graphic representation of the average cell size and SD of each cell line (Caco-2, SW480, HT-29 and RKO), being the Caco-2 the largest cells and the RKO the smallest cells.*

The nucleus-to-cytoplasm (N:C) ratio has proven to be a valuable morphologic feature, in fact it was found that the cell deformability and nucleus size are correlated, thus cells with a large and rigid nucleus are prone to be blocked by relatively narrow gaps[88,89]. For that reason, it was also relevant to perform the N:C ratio assessment, which is represented in figure 17. Interestingly, cells of smaller size such as HT-29 and RKO, presented higher N:C ratios, 0.76 and 0.83, respectively, whereas SW480 despite being larger than latter ones, has similar N:C ratio, 0.79. Lastly, Caco-2 the cell line with the smallest NC ratio, 0.67, is actually the largest in size, as summarized in table 4.

Table 4 *A summary of each CRC cell lines measurements*

Cell lines	**Caco-2** (N=21)	**SW480** (N=47)	**HT-29** (N=36)	**RKO** (N=33)
Cell diameter (µm)	22.43	17.98	13.95	13.15
Nucleus diameter (µm)	14.79	13.68	11.19	10.79
N:C ratio	0.67	0.79	0.76	0.83

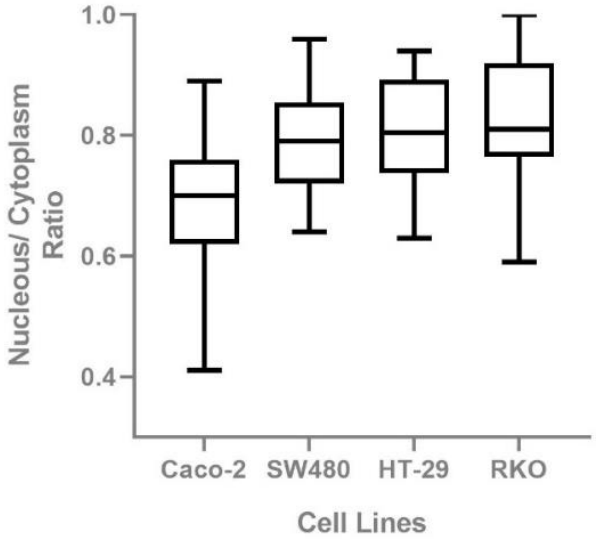

Figure 17 *Graphic representation of the Nucleus-to-Cytoplasm ratio on average and SD of each cell line (Caco-2, SW480, HT-29 and RKO).*

Considering the obtained results, the adopted flow rate for subsequent experiments and patient sample processing was 100 µL/min.

4.1.2. Optimal Capture Efficiency assessment

In order to assess the isolation efficiency of the RUBYchip™, spiking experiments with four different cell lines were performed. In these experiments, a predetermined number of 200 cultured cancer cells were spiked in a 7,5 ml whole blood sample from healthy volunteers. Thus, five different flow rates were tested, namely 80, 100, 120, 160 and 200 µL/min in order to determine the optimal flow rate, and results are presented in figure 18.

Overall, the highest capture efficiency observed was achieved at 100 µL/min consistently in all cell lines. SW480 cells reached the highest capture efficiency observed at 69.70%, followed by Caco-2 cells (60%), and finally HT-29 (10.30%). The lowest isolation efficiency observed was at 200 µL/min with an average of 17.30%, 15.10% and 1.5% of spiked SW480, Caco-2 and HT-29, respectively. Hence, 100 µL/min was selected as the optimal flow rate for subsequent sample processing.

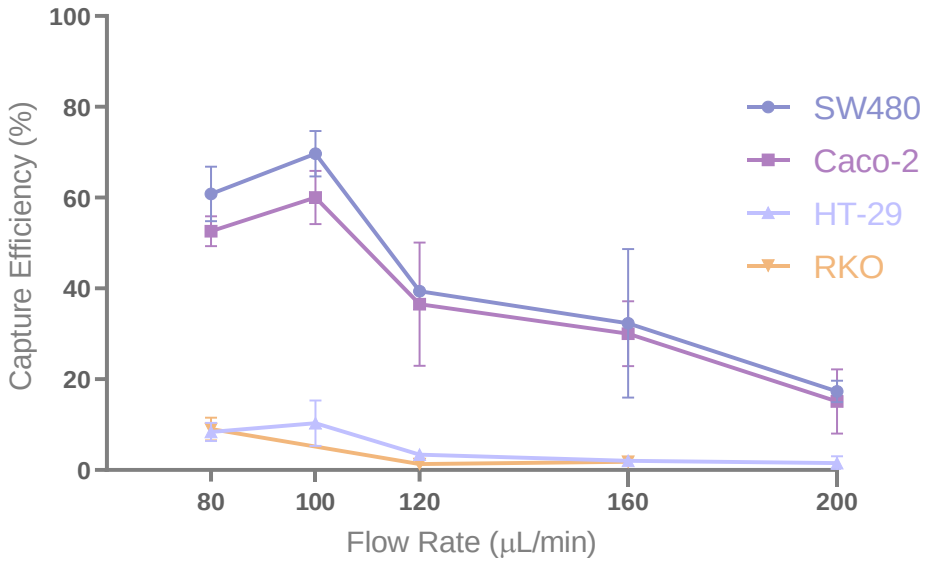

Figure 18 *Graphical representation of the isolation efficiency of the RUBYchip™ at five different flow rates, with four different cell lines, SW480, Caco-2, HT-29 and RKO. The highest results were achieved at 100 µL/min, for all the cell lines. The highest capture efficiencies,69,70% and 60%, were obtained in the largest cells, SW480 and Caco-2, respectively. For smaller cells, HT-29, the capture efficiency was lower, 10,30%.*

In these experiments, we observed highest capture efficiencies (60-70%) in cells with higher dimensions (Caco-2 and SW480), that considerably decreased in smaller cells (HT-29 and RKO). These results were consistent for all the tested flow rates in the different cell lines, which was anticipated since one of the RUBYchip™ features is size based cell capture.

It is noteworthy, that the highest capture efficiency was observed in SW480 cells, despite Caco-2 are the largest in size, which could be explained by the higher nucleus-to-cytoplasm ratio. SW480 cells present in average higher N:C ratio than Caco-2 cells, which means they are more rigid and potentially less deformable, thus more easily retained by the device.

4.1.3. Cell target influence in the Capture Efficiency

To evaluate cell target influence in the capture efficiency of the device, different cell targets (50, 200 and 1000 cells) were spiked into 7.5 mL of whole blood from healthy donors. For this experiment SW480, Caco-2 and HT-29 were used, and blood was processed at 100 µL/min, the optimal flow rate achieved in previous spiking experiments. Obtained results are represented in figure 19.

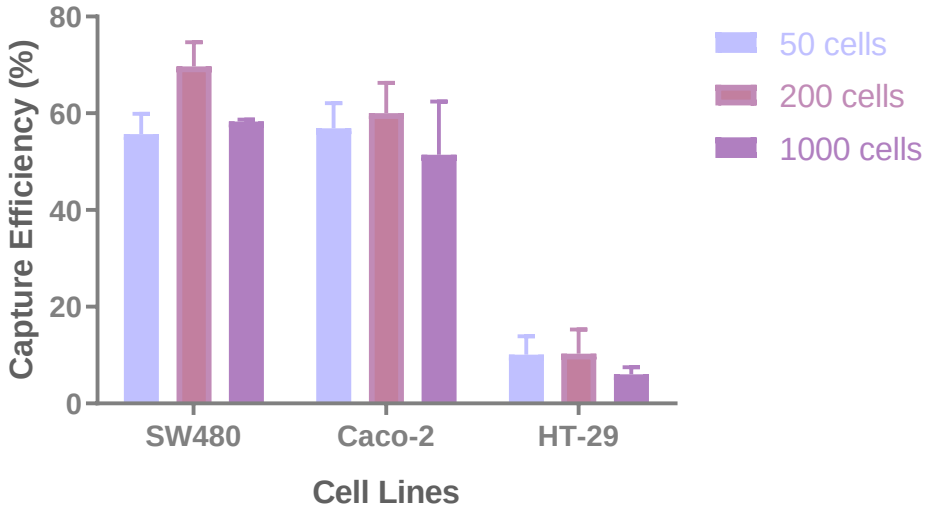

Figure 19 *Graphical representation of the capture efficiency of the RUBYchip™ with three different cell lines, SW480, Caco-2 and HT-29, varying the number of spiked cells at 100 µL/min. Capture efficiency remains high, 56%-70%, in bigger cells and decrease, 6%-10% in smaller cells.*

As it can be observed, there were not significative differences observed in the capture efficiency when changing the spiked cell target at 100 µL/min, in any of the cell lines. And it was possible to observe that the capture efficiency remains high (60-70%), for cells with higher dimensions (SW480 and Caco-2) and low (6-10%) for smaller cells (HT-29), hence suggesting that capture efficiency will be maintained equal in samples with low or high CTC content.

4.2. Optimisation and validation of cell staining and analysis

4.2.1. Immunocytochemistry optimisation in experimental samples

In order to optimise the antibody panel, biological samples (whole blood samples and isolated PBMCs) from healthy volunteers were spiked with CRC cells to mimic circulating tumour cells in patients' blood.

The antibody panel was firstly tested in adherent cells in a 24-well plate to evaluate the antibody expression in previously mentioned cell lines (SW480, Caco-2 and HT-29). In this experiments, RKO cell line was not used due to its extremely low capture efficiencies.

For the image acquisition and analysis, several parameters were firstly defined and adopted for all the following experiments to guarantee a consistent evaluation. Exposure times were established four each colour filter at 500 ms for blue, 800 ms for green, 900 ms for orange and 1s for red. Furthermore, to analyse the images and in order to obtain a clear image with maximised signal and lack of background, the lookup table (LUTs) window was adjusted for green channel (102-350), orange channel (102-400) and red channel (102-200). It is noteworthy that the following presented images of each experiment are merely representative of several observed images during the image analysis. Therefore, a much broad image repositorium exists and each image can be observed and analysed in each fluorescent filter.

The first tested antibody dilutions are expressed in table 5 and the acquired images of the first ICC experiment can be observed in figure 20. In this study, DAPI was always used in a dilution of 1:10.

Table 5 *First tested dilutions for the antibody panel and DAPI in all cultured cell lines (Caco-2, SW480 and HT-29) adhered in a 24-well plate.*

Antibody Panel		
Cytokeratin	Vimentin	CD45
Dilution		
1:200	1:50	1:100

After image analysis, it was possible to observe cytokeratin signal in all cell lines (figure 20A, E, I), which was anticipated since Cytokeratin is normally present in the cytoskeleton of epithelial cells, thus frequently used as an epithelial biomarker[90,91].

Regarding the Vimentin expression, a positive signal was only observed in SW480 cells (figure 20F), which was also expected since several studies showed vimentin expression in these cells, associated with more invasiveness and migratory properties.

In Caco-2 and HT-29 cells, the vimentin signal was absent, which was also in concordance with the literature (figure 20B, J)[92,93].

A total absence of CD45 signal was observed in all the tested cell lines. CD45 is a protein present in the membrane of the leukocytes, thus its absence on the cell lines was also expected.

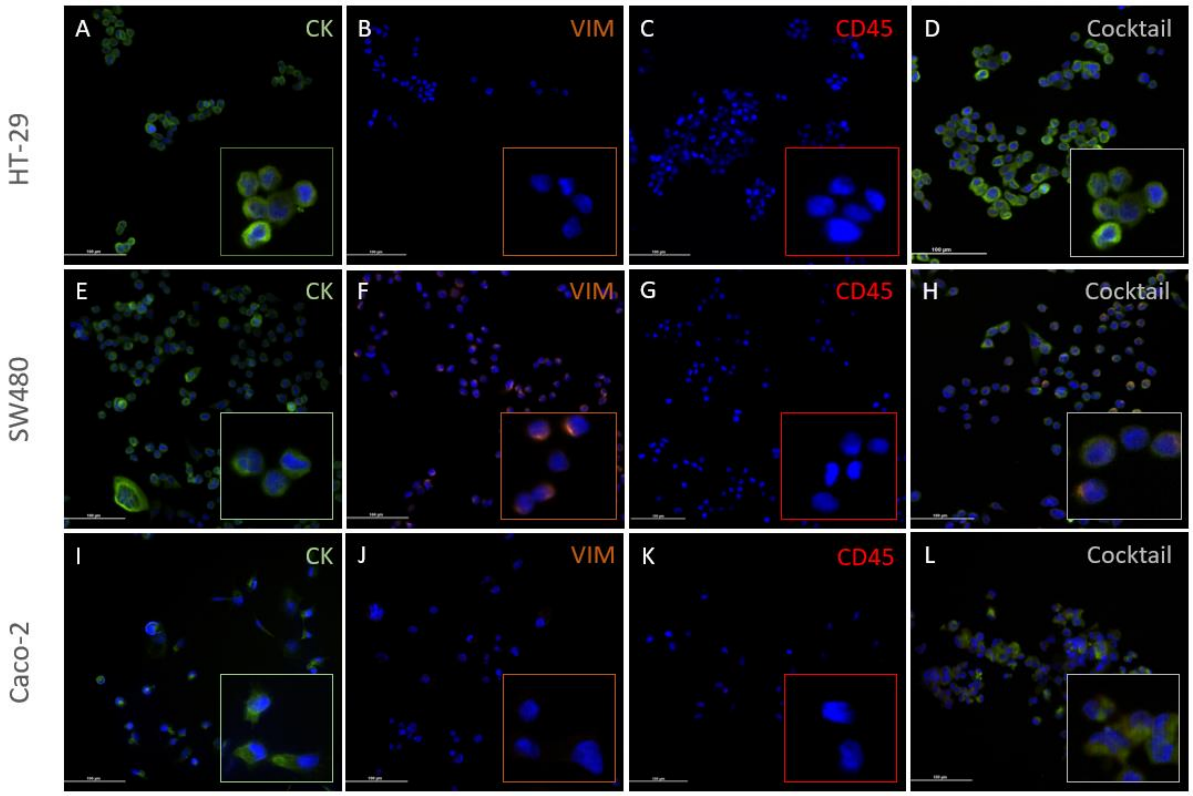

Figure 20 Immunocytochemistry performed in adherent HT-29, SW480 and Caco-2 cells. (A) CK expression (B) VIM expression, (C) CD45 expression and (D) Biomarkers expression (incubated with antibody cocktail) in HT-29 cells; (E) CK expression, (F) VIM expression, (G) CD45 expression and (H) Biomarkers expression (incubated with antibody cocktail) in SW480 cells; (I) CK expression, (J) VIM expression, (K) CD45 expression and (L) Biomarkers expression (incubated with antibody cocktail) in Caco-2 cells. DAPI is shown in all the images staining the nucleus.

Tumour heterogeneity is already very well described in the literature; hence CTCs have an important role in reflecting tumour diversity, another condition was included in this ICC, mixing all cell lines to evaluate if each cell line could be distinguished by its specific antibody combination staining. Results are showed in figure 21.

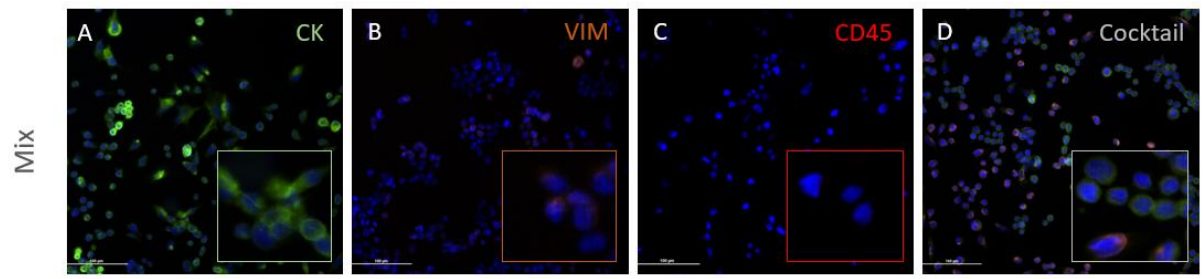

Figure 21 Immunocytochemistry of the mixed cells namely SW480, Caco-2 and HT-29 cells (A) CK expression; (B) VIM expression; (C) CD45 expression and (D) Biomarkers expression (incubated with antibody cocktail).

Interestingly, it was possible through image analysis and observation to identify each cell line based on its morphological characteristics and the specific expression of the different antibodies. The CK antibody signal was evident and very bright in HT-29 and was also observable in Caco-2 and SW480, all of them epithelial cell lines.

Furthermore, Vimentin expression, more related with a mesenchymal phenotype, was present only in SW480, which was in concordance with the previous results.

Regarding isolated PBMCs, as white blood cells, the Cytokeratin signal was expected to be absent, which was confirmed by the image analysis. The CD45 expression, which was expected to have a very clear signal, was present but a weak signal was observed, either when added alone or in cocktail, as showed in figure 22.

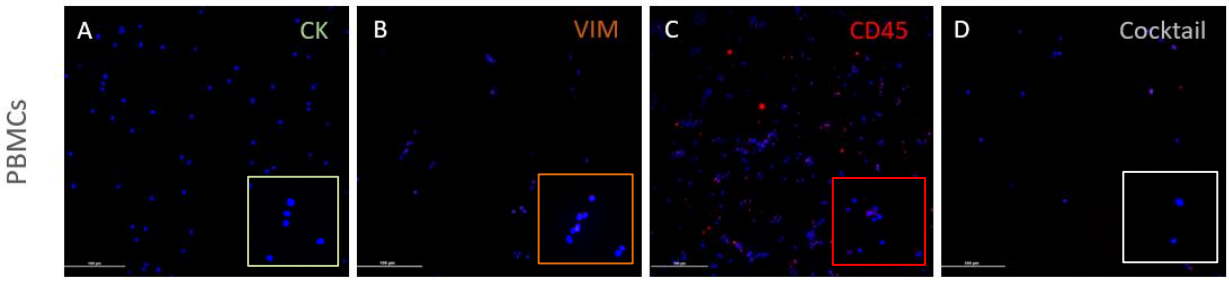

Figure 22 *Immunocytochemistry of the isolated PBMCs. (A) CK expression; (B) VIM expression; (C) CD45 expression and (D) Biomarkers expression (incubated with antibody cocktail) in PBMCs.*

Once achieved the logical antibody panel optimization in the most standardized way, the next natural step would be to proceed optimisation under the conditions that are closer to the patient sample processing. Thus, it was relevant to test selected antibodies conditions together with the cells of interest in the same device intended to be used for the clinical samples. Understandably, this implies testing antibody panel in blood samples alone and testing the antibody panel in spiked samples which are run in the RUBYchip™.

Additionally, inside this device all cell populations are in suspensions and unevenly distributed along the microchannels, which poses different technical challenges from the well-plate static conditions.

CD45 is an extracellular protein expressed in leucocytes membrane, hence cell permeabilization prior to antibody addition is not necessary. However, since the device is aimed for high throughput applications, a more suitable protocol must be adopted. For that reason, two different negative control conditions were tested, namely i) a step-by-step protocol in which CD45 was incubated first, then cell membrane permeabilization was performed, followed by incubation with the other antibodies (CK and VIM); ii) a single

step incubation protocol with a cocktail of antibodies, in which antibodies were added in one solution with previous cell permeabilization and, subsequently incubated for one hour and fifteen minutes.

Image analysis and acquisition was obtained in the same conditions of exposure times, and LUTs window, as previously described and the acquired images are showed in figure 23.

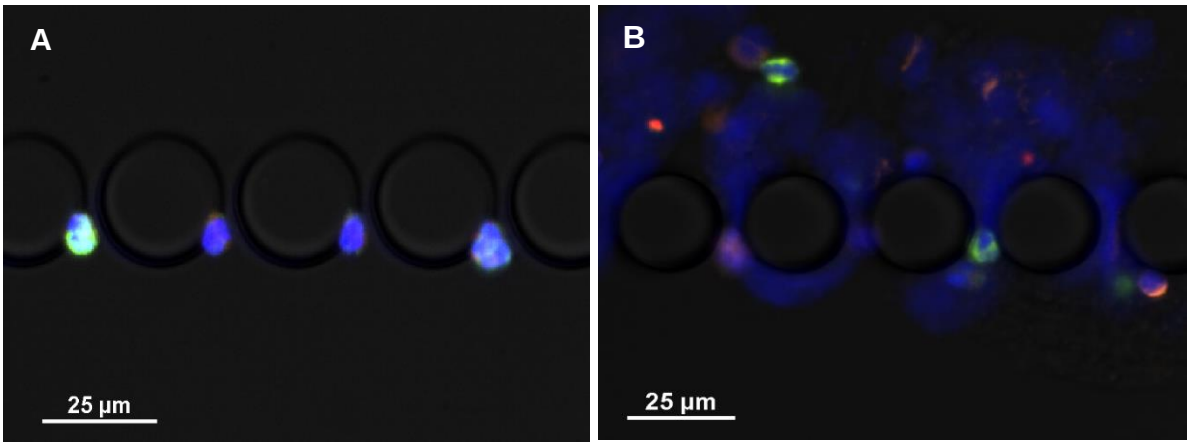

Figure 23 *Immunocytochemistry assay to evaluate two different protocols in whole blood samples from healthy donors (A) antibodies added in a single-step (cocktail) versus (B) antibodies added step-by-step.*

When comparing both protocols, there was no significative differences observed between both protocols regarding antibody expression, therefore the cocktail of antibodies procedure was adopted for the following experiments since it allows a quicker protocol.

Furthermore, in this experiment it was possible to observe Cytokeratin expression in white blood cells, which was not supposed to be occurring, such lack of specificity may be indicative that the antibody dilution tested is not ideal. For that reason, first a whole blood sample from healthy volunteers spiked with SW480 cells was processed and stained in the device with the same dilutions tested in previous experiments with adherent cells (table 5). Acquired images are presented in figure 24.

As expected, it was possible to observe a bright Cytokeratin signal in SW480 cells, however a weaker unspecific signal was also observed in the white blood cells. Regarding Vimentin expression, a very weak signal was observed when compared to previous observations in adherent cells. CD45 signal was positive only in white blood cells, as anticipated.

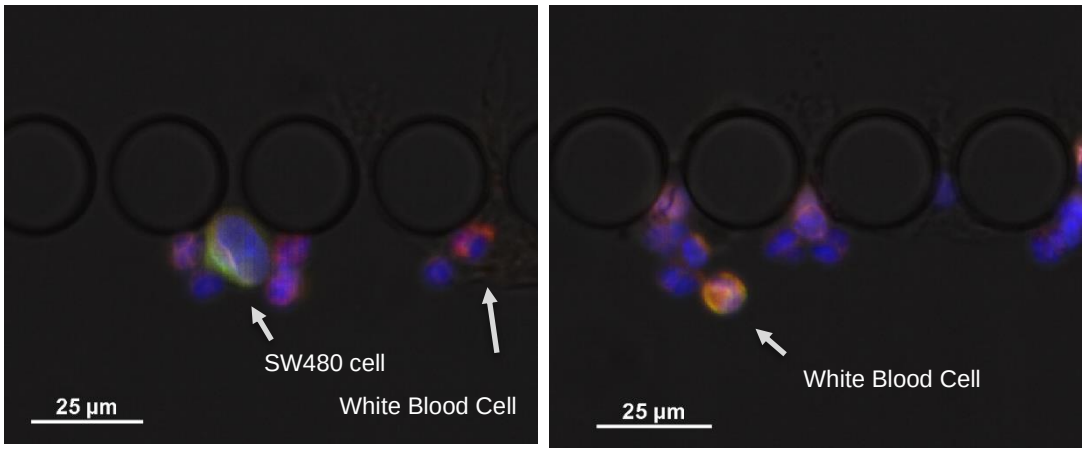

Figure 24 *Immunocytochemistry assay for antibodies optimisation in whole blood sample from healthy volunteers spiked with SW480 cells and stained with the cocktail of antibodies and DAPI.*

To better explore the lack of specificity, the anti-CK antibody was used in the same antibody cocktail but further diluted compared to the previous experiment, as presented in table 6. However, in this assay, the PBMCs were added along with the cells in each tested condition to better mimic what happens inside the device where the cancer cells are in direct contact with the blood cells.

Table 6 *Second tested dilutions for the antibody panel and DAPI in all cultured cell lines (Caco-2, SW480 and HT-29) adhered in a 48-well plate. CK antibody was diluted to 1:500.*

Antibody Panel		
Cytokeratin	Vimentin	CD45
Dilution		
1:500	1:50	1:100

As expected, all cell lines showed CK signal (figure 25A, D, G), which is absent in the surrounded PBMCs. Similarly to what was observed in previous experiments, SW480 cells presented vimentin signal, however it seemed to be also present in the PBMCs (figure 25B, E, H). Indeed, several studies have been demonstrated the presence of the intermediate filament protein vimentin on the surface of activated platelets, lymphocytes and neutrophils[94–96].

However, it was also possible to observe a CD45 antibody signal in larger cells, morphologically consistent with cultured CRC cells, which was not expected. Since cultured cells do not express CD45, this is indicative of unspecific binding of the CD45

antibody, thus this results should be further repeated. Regarding the PBMCs, the CD45 signal was very weak, contrary to what was expected.

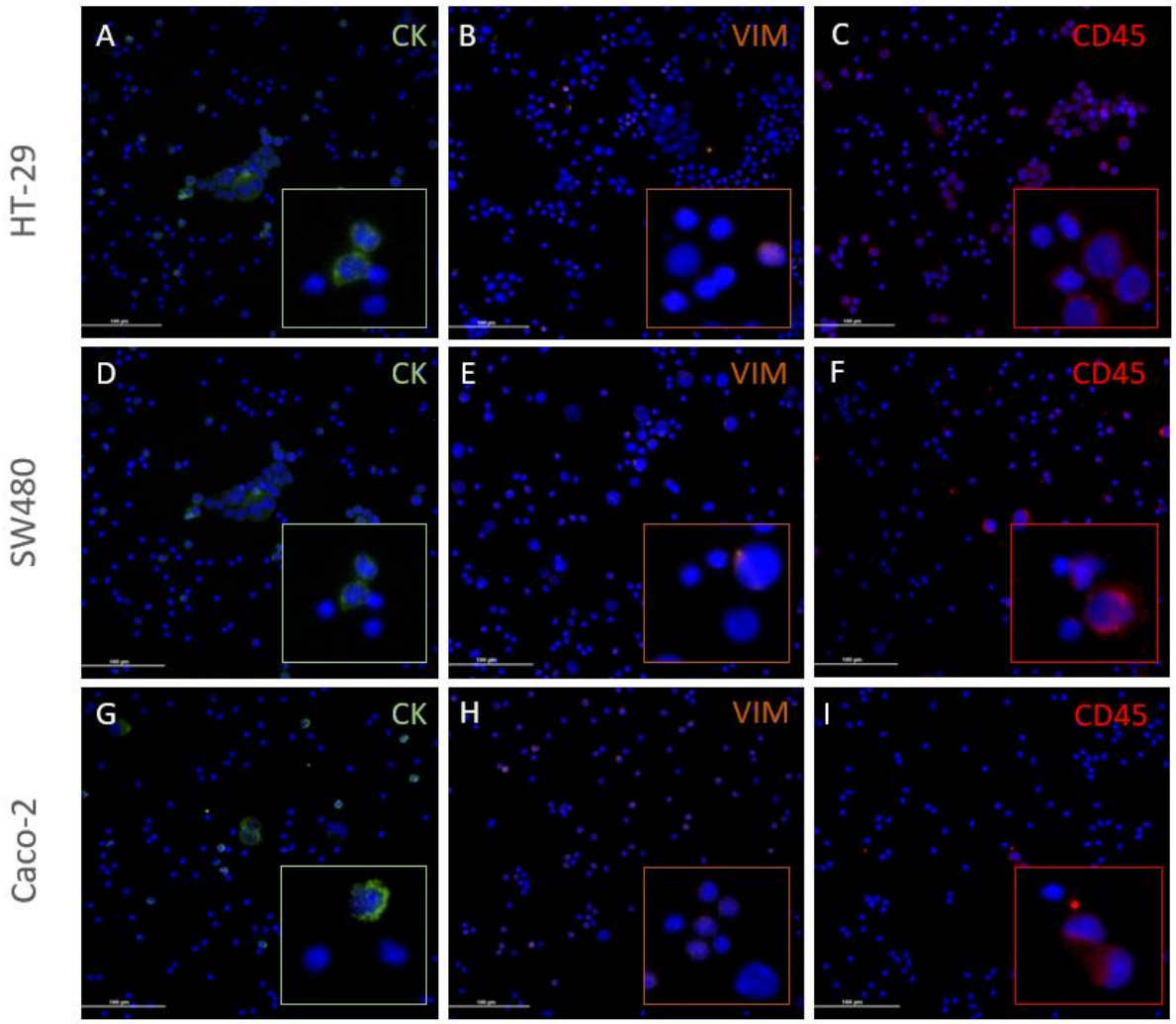

Figure 25 *Immunocytochemistry in 48-well plate of HT-29, SW480 and Caco-2 cells along with PBMCs (A) CK expression (B) VIM expression, (C) CD45 expression of HT-29; (D)CK expression (E) VIM expression and (F) CD45 expression of SW480 cells; (G) CK expression (H) VIM expression and (I) CD45 expression of Caco-2 cells.*

As in the previous assay, a mix containing all the cultured cell and the PBMCs was performed, as illustrated in figure 26. The results showed the expectable regarding the Cytokeratin and Vimentin expression. Cytokeratin was observed in all cultured CRC cells (figure 26A) and Vimentin was only expressed by SW480 cells (figure 26B).

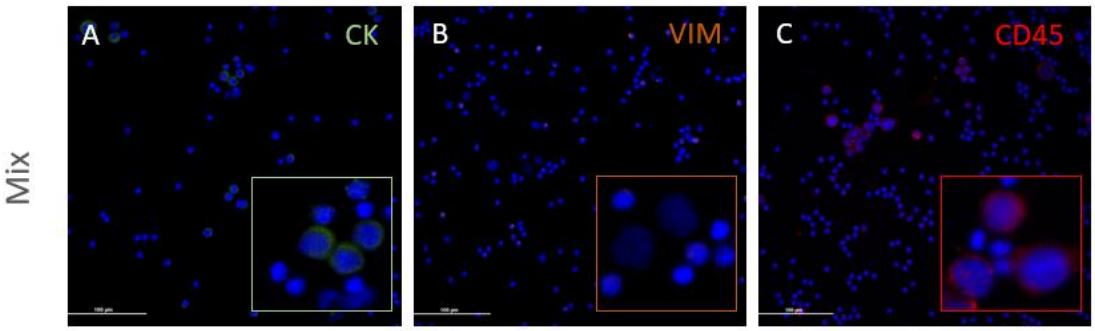

Figure 26 *Immunocytochemistry in mixed cell lines and PBMCs. (A) CK expression; (B) VIM expression; (C) CD45 expression.*

However, unexpected results were observed regarding CD45 expression, since CD45 signal was not only faint in the PBMCs but was also present in cultured cells (figure 26C). This led us to hypothesize that this finding was associated with technical issues, since cultured cells do not express CD45 biomarker, as previously discussed.

Even though some findings were not as anticipated, ICC experiments proceeded in the device, using the same antibodies and the same antibodies dilutions, in order to seek a clear answer. In the experiments performed in device, two different conditions were tested, as detailed in table 7.

Table 7 *Tested dilutions of the antibody panel and DAPI applied in two different experimental sets.*

Cocktail of antibodies (CK 1:500, VIM 1:50, CD45 1:100)	Spiked SW480 cells	Isolated PBMCs
		Whole Blood sample

On one hand, a whole blood sample from a healthy donor was spiked with SW480 cells and then passed through the device. On the other hand, PBMCs were isolated from a whole blood sample and next spiked with SW480 cells and subsequently processed in the device. Both to be further stained with the cocktail of antibodies. Obtained images are presented in figure 27.

Comparing both ICCs, it was observed that in the whole blood sample, the CK signal had higher intensity. Vimentin expression was also observed in SW480 cells in both ICCs, which was expected. With respect to CD45, in both settings, signal is present not only in the blood cells, as predicted, but also in the SW480 cells, which could be related to non-specific binding of the antibody.

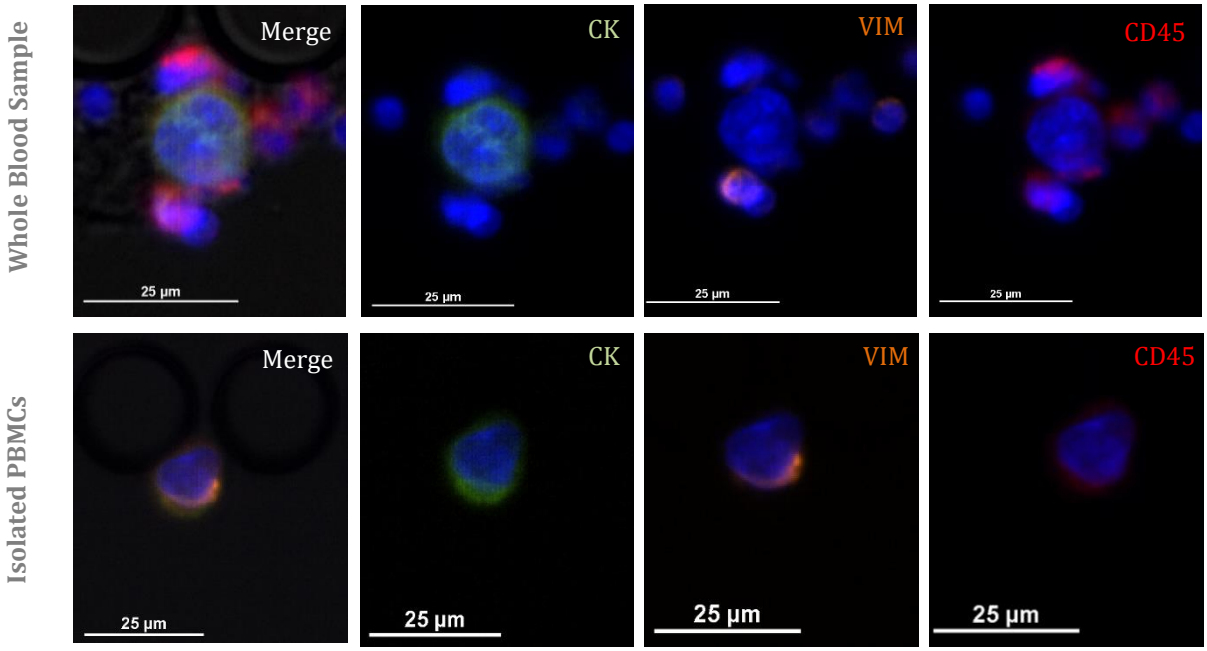

Figure 27 *Immunocytochemistry performed in a whole blood sample spiked with SW480 cells (top) and in PBMCs isolated from blood samples from healthy volunteers spiked with SW480 cells (bottom) and then stained with the cocktail of antibodies.*

To better understand the lack of CD45 and CK specificity, additional experiments without spiked cells were performed as negative controls. Whole blood samples from healthy volunteers and, at the same time, PBMCs isolated from whole blood samples of healthy donors were processed in the device, stained, and analysed in the same conditions as the previous experiments and are exposed in table 8.

Table 8 *Different experimental conditions for the antibody panel testing. Each treated with different antibodies conjugations in either whole blood samples or isolated PBMCs.*

Cocktail of antibodies (CK 1:500, VIM 1:50, CD45 1:100)	Whole Blood Sample Only
	Isolated PBMCs Only
CK alone (CK 1:500)	Whole Blood Samples Only
	Isolated PBMCs Only
Without CK (VIM 1:50, CD45 1:100)	Whole Blood Sample Only

Regarding CD45 antibody signal, it was present in white blood cells in both ICCs, however the signal intensity was variable and, brighter in the whole blood sample (figure 28A, C). Consistently with previous observations, Cytokeratin signal was found in white blood cells in both samples, either whole blood and isolated PBMCs (figure 28B, E), although signal is very weak and much contrasting with clear signal previously found in biological positive events, like spiked SW480 cells, so easily distinguished from unspecific binding to WBCs.

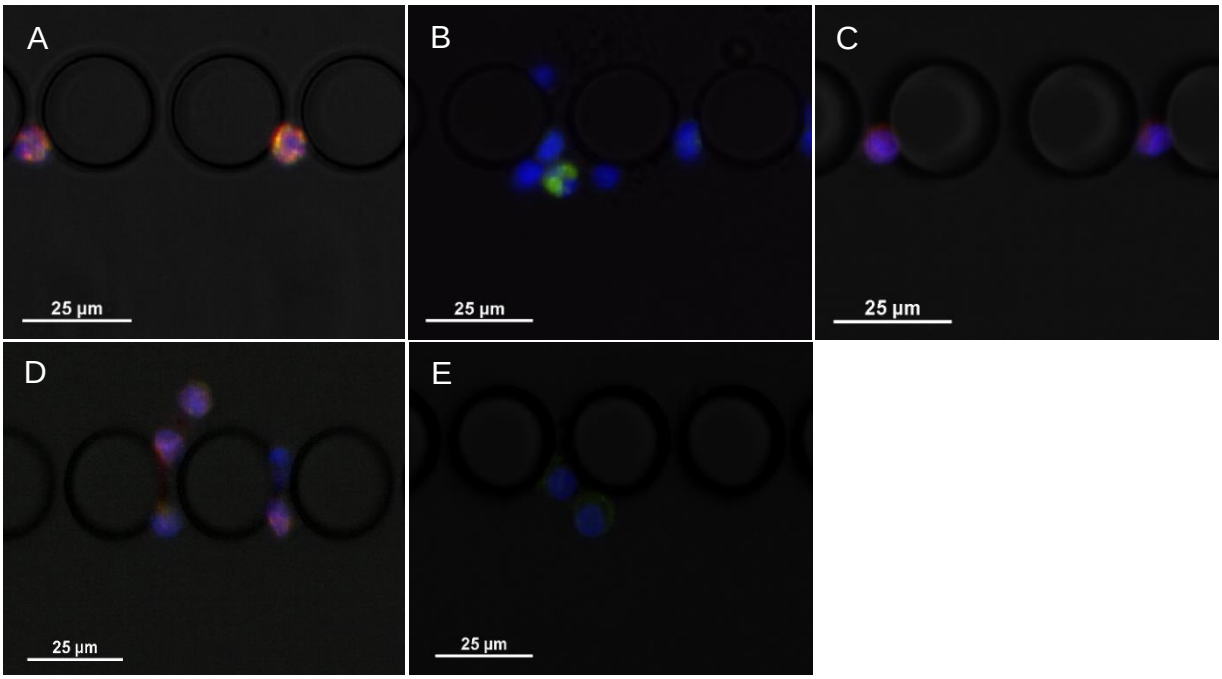

Figure 28 *Images obtained from the immunocytochemistry assays using whole blood samples (top) or isolated PBMCs (bottom). (A) Whole blood sample stained with the cocktail of antibodies; (B) Whole blood sample stained with Cytokeratin alone and (C) Whole blood sample stained without Cytokeratin (Vimentin and CD45 antibodies); (D) Isolated PBMCs stained with the cocktail of antibodies and (E) Isolated PBMCs stained with Cytokeratin alone*

This results leads us to believe that this weaker signal could be related to non-specific binding or a possible sub-population of cells that express some of the Cytokeratins recognised by the pan-Cytokeratin antibody used, which needs further in depth studies. However, since the identification of CTCs in the device relies on the biomarkers expression, and in order to eliminate any doubts regarding the antibody's specificity, a different Cytokeratin and CD45 antibodies were tested, these new antibodies were purchased from a different companies than previous ones (see table 2 in section 3.4 of the Materials and Methods).

Firstly, and similarly to the previous ones, they were tested in the same adherent cells on a 24-well plate in the dilutions expressed in table 9.

Table 9 *First tested dilutions for the antibody panel, with newly acquired CK and CD45 antibodies in all cultured cell lines (Caco-2, SW480 and HT-29) adhered in a 24-well plate.*

Antibody Panel		
Cytokeratin	Vimentin	CD45
Dilution		
1:75	1:50	1:100

Once again, the image acquisition and analysis followed the same conditions as the ones previously mentioned and they are illustrated in figure 29.

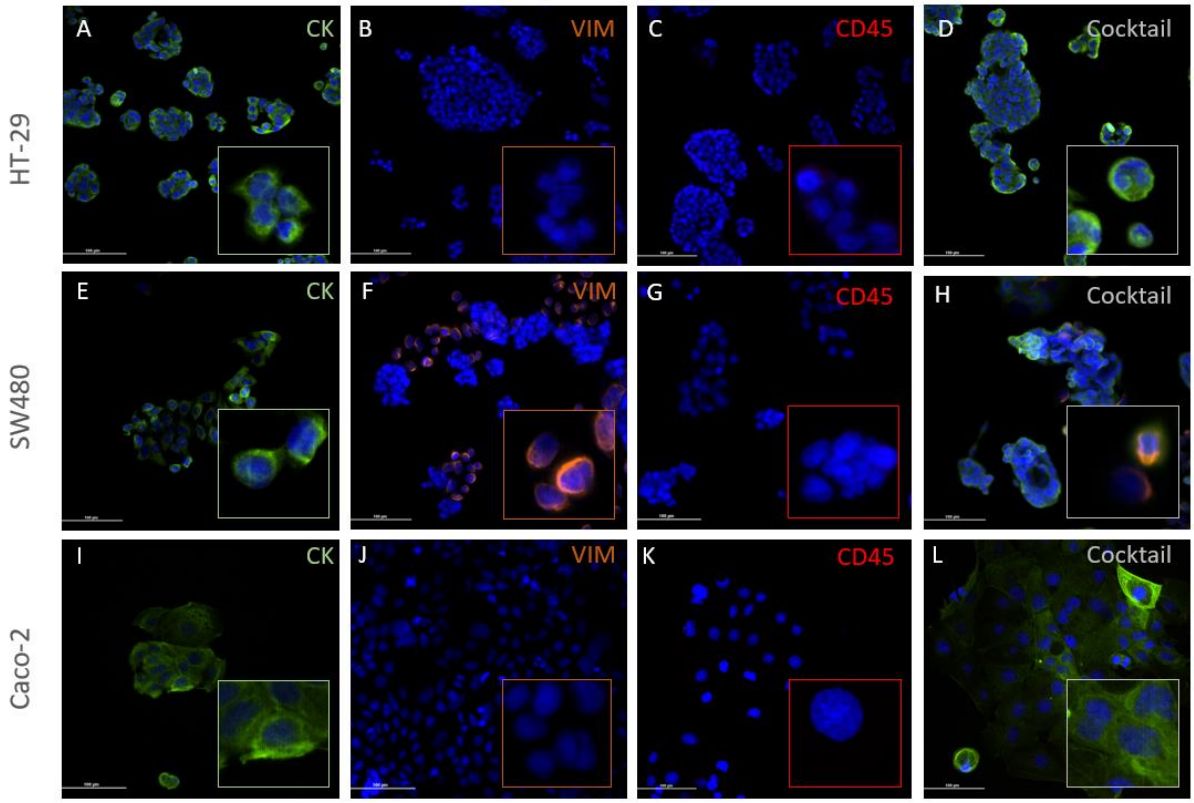

Figure 29 *Immunocytochemistry of adherent HT-29, SW480 and Caco-2 cells. (A) CK expression (B) VIM expression, (C) CD45 expression and (D) Biomarkers expression (incubated in cocktail) in HT-29 cells; (E) CK expression, (F) VIM expression, (G) CD45 expression and (H) Biomarkers expression (incubated in cocktail) in SW480 cells; (I) CK expression, (J) VIM expression, (K) CD45 expression and (L) Biomarkers expression (incubated in cocktail) in Caco-2 cells. DAPI is shown in all the images staining the nucleus.*

As expected, Cytokeratin expression was observed in all cell lines very brightly. Regarding the Vimentin expression, and similarly to what was already demonstrated, only SW480 cells presented positive signal for the same reasons already pointed out. Finally, CD45 signal was absent in all cell lines as expected since they are specific to white blood cells.

Considering these positive results, this antibody panel was further tested in the RUBYchip™ at different dilutions since signal expression could be slightly distinct. Thus, the tested dilutions are presented in table 10.

Table 10 *Tested dilutions for the newly acquired antibodies, in whole blood samples from healthy volunteers spiked with SW480 cells and processed in the RUBYchip™.*

Antibody Panel				
Cytokeratin		Vimentin	CD45	
Dilutions				
1:75	1:100	1:50	1:50	1:100

Firstly, the newly acquired CD45 (SC, 1:100) was tested in a cocktail together with the previous cytokeratin (Sigma, 1:500) in i) a whole blood spiked with SW480 cells, ii) in a whole blood sample alone and iii) in isolated PBMCs from healthy volunteers. The obtained images are illustrated in figure 30.

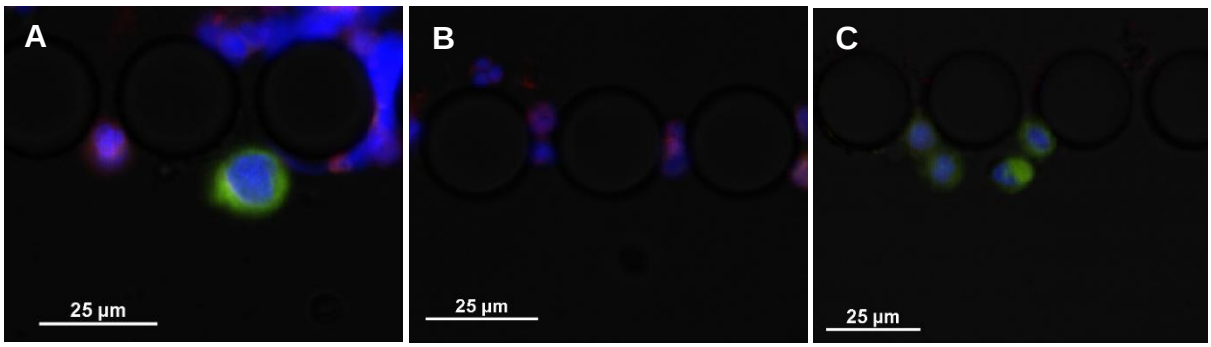

Figure 30 *Immunocytochemistry images obtained from a (A) whole blood sample spiked with SW480 cells, (B) a whole blood sample alone and (C) in isolated PBMCs only. All of them stained with the cocktail of antibodies composed by the old cytokeratin, the vimentin and the new CD45.*

By image analysis, it was possible to observe a positive CD45 signal restricted to the white blood cells (figure 30A, B) and PBMCs (figure 30C) and a total absence in the cell lines, which lead us to assume that this antibody appeared to be more specific than the one previously tested. Nevertheless, in some cases CD45 signal was weak, so in the following experiments a dilution of 1:50 was tested, to evaluate if a brighter signal was obtained.

Regarding the Cytokeratin signal, it was very bright in SW480 cells (figure 30A), however it was still possible to observe a weak signal in the white blood cells (figure 30B) and a bright signal in the PBMCs (figure 30C).

For that reason, a newly acquired Cytokeratin antibody was tested in a cocktail of antibodies composed by the new CD45 and the Vimentin in a whole blood sample, from healthy volunteers, spiked with SW480 cells in a dilution of 1:100 of Cytokeratin and 1:50 of CD45. The obtained images are presented in figure 31.

Regarding Cytokeratin signal, it was possible to observe a very specific signal restricted to the spiked SW480 cells, however the intensity signal was weak, so we decided to increase the concentration in the following experiments. CD45 signal was very bright and also very specific to the white blood cells.

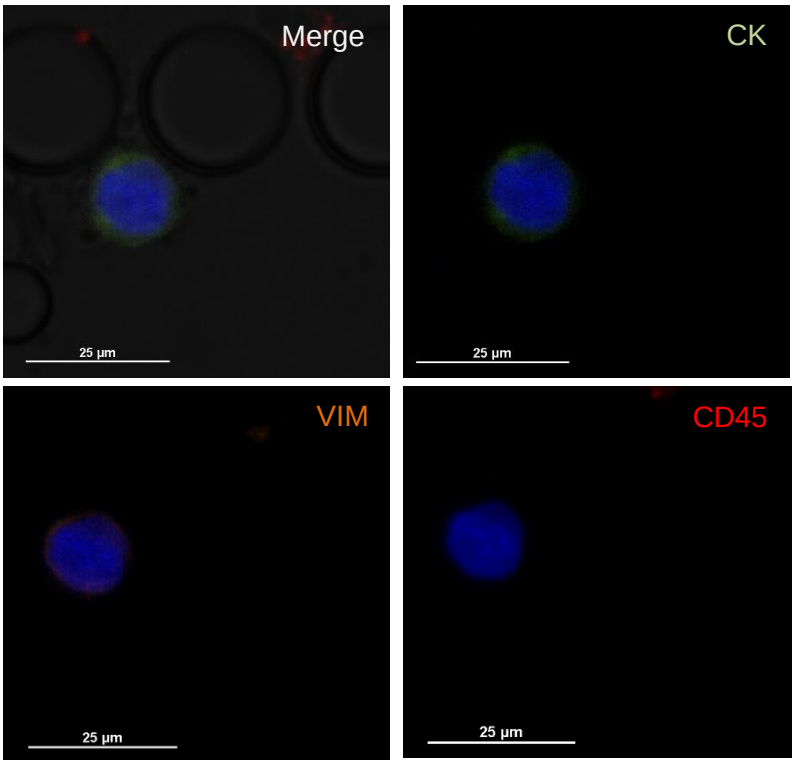

Figure 31 *Immunocytochemistry images obtained from a whole blood sample spiked with SW480 cells stained with the cocktail of antibodies composed by the newly acquired Cytokeratin (Exbio, 1:100), the Vimentin and the newly acquired CD45 (SC, 1:50).*

A last ICC experiment was performed in a whole blood sample from a healthy volunteer spiked with SW480 cells to evaluate a different Cytokeratin dilution (1:75), and obtained images are presented in figure 32. Finally, in these dilution Cytokeratin signal was brighter than in previous experiments. Although in this experiment Cytokeratin expression was specific to the SW480 cells, as we expected it would be, the intensity signal is not ideal yet.

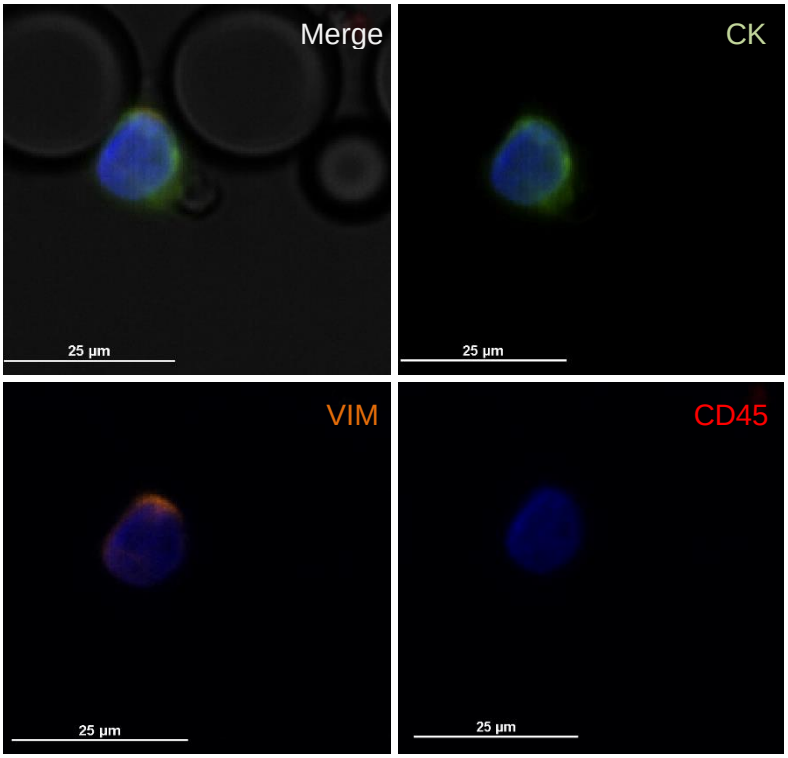

Figure 32 *Immunocytochemistry images obtained from a whole blood sample spiked with SW480 cells stained with the cocktail of antibodies composed by the new Cytokeratin (1:75), the Vimentin and the new CD45 (1:50).*

In the following scheme (figure 33), it is possible to observe a summarized representation of ICC experimental design.

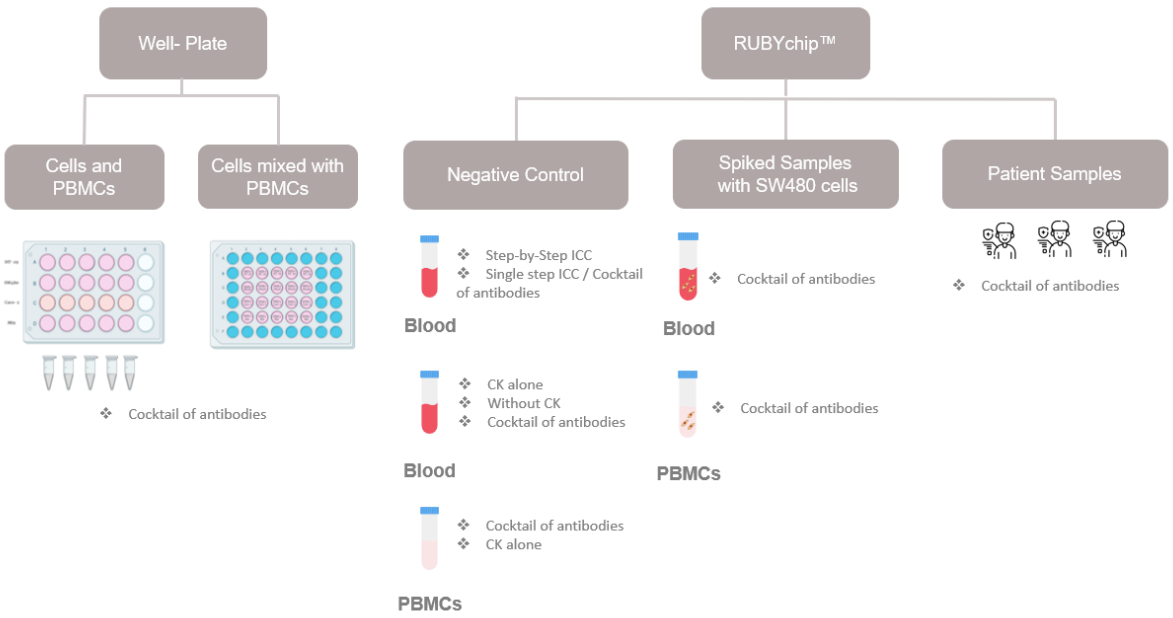

Figure 33 *Schematic representation of ICC experimental design*

All ICC experiments are summarized in the following table (table 11).

Table 11 *Summarize table of all ICC experiments*

Experiment	Platform	Sample	Antibody dilutions	Results	Next Step
1 Evaluate antibody panel expression in cell lines and PBMCs	Plate	Cells and PBMCs	CK 1:200 VIM 1:50 CD45 1:100	• CK expression in cultured cell lines • VIM expression in SW480 cells • CD45 signal absence in cultured cell lines • Weak CD45 signal in PBMCs	• Test the antibody panel in the device at the same dilutions
2 **Negative Control** To compare two different protocols	Device	Only Blood	CK 1:200 VIM 1:50 CD45 1:100	• No significant differences were found between protocols	• Test antibody cocktail in spiked samples, same Ab dilutions
3 Evaluate antibodies dilution in spiked samples	Device	Spiked blood	CK 1:200 VIM 1:50 CD45 1:100	• Bright CK signal in SW480 cells • However, CK expression in WBCs	• Test diluted CK ab and check its expression in cell lines with PBMCs
4 Evaluate CK expression in 1:500 dilution	Plate	Cells mixed with PBMCs	CK 1:500 VIM 1:50 CD45 1:100	• Clear CK signal in cultured cell lines • CK expression absent in WBCs • CD45 signal observed in cultured cell lines and quite weak in PBMCs	• Test different conditions in device using the same antibody dilutions
5 **Negative Control** To evaluate CK and CD45 expression in isolated PBMCs	Device	Only PBMCs	CK only 1:500 CK 1:500 VIM 1:50 CD45 1:100	• CD45 signal was observed in the isolated PBMCs • CK signal was also observed in the PBMCs	• Test the same conditions in blood samples only
6 **Negative Control** To evaluate CK and CD45 expression in blood samples	Device	Blood only	CK only 1:500 Without CK VIM 1:50 CD45 1:100 CK 1:500 VIM 1.50 CD45 1:100	• Although in a faint signal, CK signal was observed in WBC • Antibodies signal as expected • CK signal was also observed in WBC	• Test the same Ab dilutions in spiked samples
7 To evaluate CK and CD45 expression (in the same dilutions) in spiked samples	Device	Spiked Blood Spiked PBMCs	CK 1:500 VIM 1:50 CD45 1:100	• CK expression in SW480 cells • CD45 signal was generally faint and was observed in SW480 cells	• Test a new CD45 antibody (SC) and a new Cytokeratin antibody (Exbio) both in cells lines and in isolated PBMCs
8 Evaluate Ab panel in cell lines and PBMCs	Plate	Cell lines and PBMCs	CK (Exbio) 1:75 VIM 1:50 CD45 (ST) 1:100	• CK expression in all cell lines • VIM expression only in SW480 cells • CD45 signal absent in all cell lines • CD45 signal in PBMCs	• Test the new Ab in the device
9 **Negative Control** To evaluate the new CD45 (SC) antibody	Device	Blood only PBMCs only	CK 1:500 VIM 1:50 CD45 (ST) 1:100	• CD45 expression was very specific in both samples, however a weak signal was observed	• Test the same Ab dilutions in spiked samples
10 Evaluate Ab panel, combining the old Cytokeratin (CK) with the new CD45 (SC)	Device	Spiked Blood	CK 1:500 VIM 1:50 CD45 (ST) 1:100	• CD45 expression only in WBC • CK expression observed in SW480 cells and in some punctual cases of WBC	• Test all the new Ab (CK Exbio and CD45 SC), in cocktail, in spiked samples • Decrease CD45 (SC) dilution
11 Evaluate the new Ab panel	Device	Spiked Blood	CK (Exbio) 1:100 VIM 1:50 CD45 (SC) 1:50	• CD45 signal was observed very brightly in WBC • CK expression was weak in cell lines • CK and CD45 co-expression	• Increase CK (Exbio) dilution
11 Evaluate a different dilution for CK (Exbio)	Device	Spiked Blood	CK (Exbio) 1:75 VIM 1:50 CD45 (SC) 1:50	• Cytokeratin signal was better, but still weak compared to the first Cytokeratin antibody used	• Proceed to patient samples

4.2.2. Immunocytochemistry Validation in Clinical Samples

After testing the antibody panel on the RUBYchip™ in mimetic conditions using CRC cell lines, a last optimization experiment was performed in whole blood samples from metastatic colorectal cancer patients. Three different mCRC samples (P1, P2, P3) were used for further validation of previous findings.

Patient information are detailed in table 12.

Table 12 *Colorectal Cancer patients' information and tested antibody panel.*

Patient	Cancer Type	Stage	Metastasis location
P1	Colorectal Cancer	T3N+M0	• Lymph nodes spread
P2		T4aN2M0	• Metachronous liver metastasis
P3		TxNxM1	• Liver metastasis • Suspicion of pulmonary metastasis

In order to evaluate antibodies specificity in patient samples, different antibodies combinations were used to stain the patient samples and further proceed with analysis and CTC enumeration. Patient 1 whole blood sample was stained with Cytokeratin (Sigma, 1:200), Vimentin (1:50) and CD45 (Immunostep, 1:100), the first tested antibodies and respective dilutions tested in previous ICC assays. Regarding CD45 expression, it was possible to observe a very bright signal in white blood cells, as expected. Vimentin expression was also observed in a considerable number of events, some of them co-localized with Cytokeratin. It was also possible to observe Cytokeratin signal in white blood cells, which may be indicative that there was an unnecessary high concentration of the antibody tested, hence increasing the dilution could be a logical next step in further optimizing. Proceeding with CTC enumeration, it was possible to find a total of 35 CTCs, from which 30 were of mesenchymal phenotype (VIM^+, $CD45^-$) and 5 of EMT phenotype (CK^+, VIM^+, $CD45^-$), as shown in figure 34. No CTC with epithelial phenotype was found in this patient sample, all observed Cytokeratin positive cells (CK^+/VIM^- and/or CK^+/VIM^+) were also positive for CD45, hence excluded as CTC.

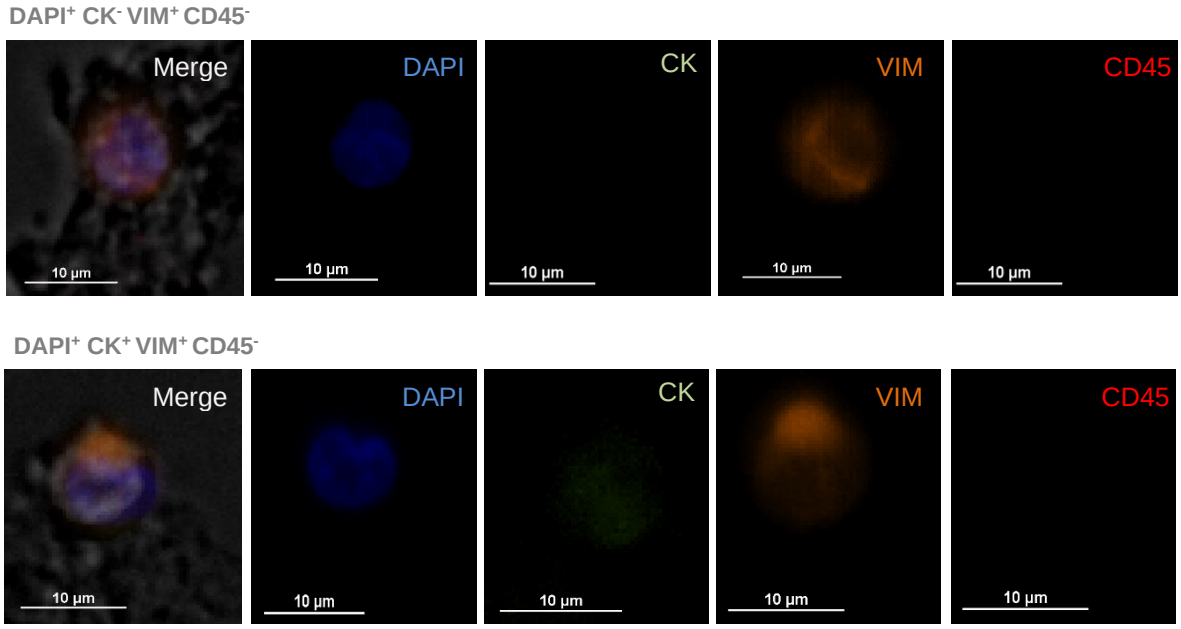

Figure 34 *Images obtained in the immunocytochemistry assay performed in the blood sample from P2. On top a CTC event with a mesenchymal phenotype characterized by an expression of Vimentin and absence of Cytokeratin and CD45 ; On the bottom, CTC event with an epithelial-mesenchymal phenotype characterized by a simultaneously expression of Cytokeratin and Vimentin and total absence of CD45 signal.*

Considering Patient 2 whole blood sample, the staining was performed with newly acquired antibodies, namely Cytokeratin (Exbio, 1:75) and CD45 (Santa Cruz, 1:50), and Vimentin (1:50). Consistent to previous ICC experiments, the newly acquired CD45 signal was very bright and specific to the white blood cells, therefore this antibody was adopted for the following assays. Considering Vimentin expression, in this sample, very few events were observed. By image analysis, it was possible to observe a weak Cytokeratin signal co-expressed with a bright CD45 signal (CK^+, $CD45^+$), thus these very few events were excluded as CTCs. All observed Cytokeratin and/or Vimentin positive cells (CK^+/VIM^-, CK, VIM^+ and/or CK^+/VIM^+) were also positive for CD45, hence excluded as CTC, which means no CTC was found in this patient sample.

Finally, concerning Patient 3, duplicate samples (S1 and S2) were obtained, since two tubes were collected in the same blood draw. Thus, whole blood samples were processed at the same time in two separate devices to be stained with different Cytokeratin antibodies. Sample 1 was stained with the newly acquired CK (Exbio, 1:75) and Sample 2 was stained with CK (Sigma, 1:500). They were both stained with the newly acquired CD45 (Santa Cruz, 1:50), which proved to be more specific in the assays previously performed, and Vimentin (1:50), incubated as usual in a single step, in cocktail.

In subsequent image analysis, similar to previous findings, CD45 signal was very bright and highly specific to white blood cells in both samples. Regarding Vimentin expression, all positive events found, in both samples, were excluded as CTCs since they also were CD45 positive. It was also possible to observe a brighter Cytokeratin signal in S2, where using CK antibody (Sigma, 1:500) than in S1, with CK antibody (Exbio, 1:75). Additionally, it was also possible to observe Cytokeratin and CD45 co-expression in cell-like events, in both samples (S1 and S2), which could represent white blood cells staining non-specifically with CK and/or CTC staining non-specifically with CD45. Either way and regardless of CD45 signal intensity, these events (CK^+, $CD45^+$) were always excluded as CTCs. These $CK^+/CD45^+$ events have been reported in other technologies described in the literature[97,98]. In Sample 1 no CTC was found, whereas two epithelial CTCs were found in Sample 2, as exhibited in figure 35.

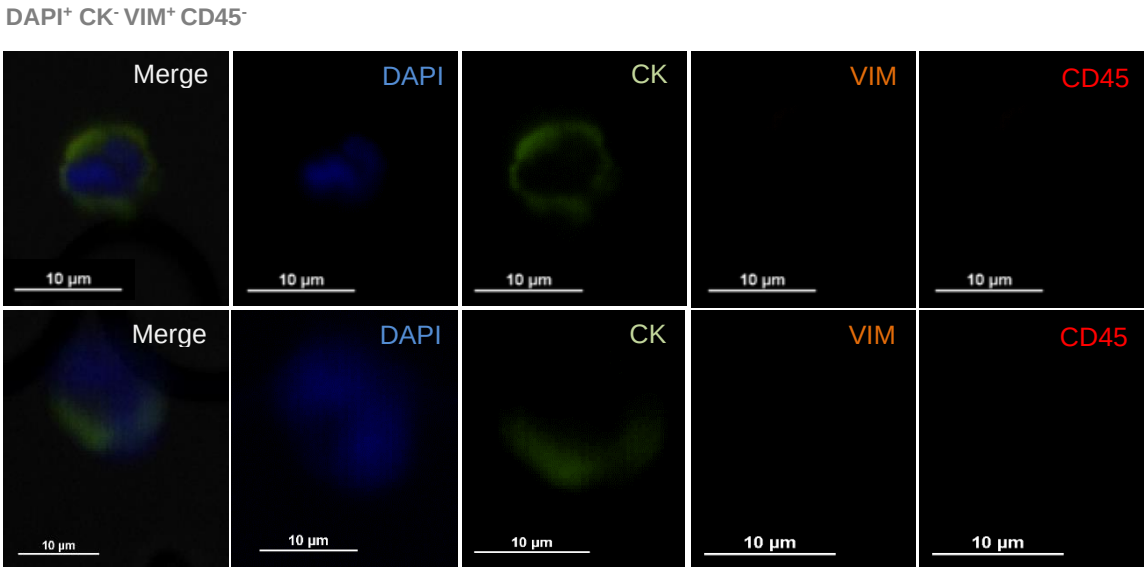

Figure 35 *Images obtained in the immunocytochemistry assay performed in Sample 2 from Patient 3. Two different CTC events with an epithelial phenotype (CK^+, VIM^-, $CD45^-$), characterized by Cytokeratin expression and total absence of Vimentin and CD45 expression.*

As mentioned, Sample 1 and Sample 2 were stained with two distinct Cytokeratin antibodies, and different dilutions as well, hence not immediately comparable in regard to CTC enumeration. Additionally, it would be understandable to find discrepancies within reason in CTC enumeration in separate 7.5 mL whole blood samples. This highlights the relevance in conducting extensive optimization studies regarding this methodology for the isolation and identification of CTCs.

The use of antibodies to identify antigens in cells and tissues has long been one of the most powerful and popular tools in cell biology. Particularly in CTC isolation technologies, the use of biomarkers for the identification and enumeration of candidate CTCs has been uniformly used. Indeed, the theory is very clear the antibody is supposed to bind to its specific antigen, like a key fits a lock. Therefore, it should be technically straightforward to add the antibody to a particular section of cells and identify unequivocally where the antibody binds, which means where its specific antigen is localized[99,100]. Yet, this complex biological binding could lead in some cases to lack of specificity and sensitivity.

There is a clear benefit of CTCs immunological staining, however it is also important to have in consideration the bioimaging equipment for CTC analysis. In this study, the microscope used to carry out image acquisition and analysis is a broad application tool, which has limitations concerning focal plane, filter set, large scan imaging, among others, which impacts image quality and resolution. Overall, it would be ideal for this purpose to use an equipment specifically developed for CTC imaging and analysis, with such an equipment, imaging CTC candidate would be done in a more accurate, feasible and fast manner.

5. Conclusion and Future Perspectives

Circulating tumour cells have gained much attention in the field of cancer research. Indeed, these cells can serve as a functional biomarker and as a potential tool in the study of metastasis. Hence, the purpose of this work was to optimise and validate a microfluidic device, the RUBYchip™, for the isolation and characterization of circulating tumour cells from whole blood samples in metastatic colorectal cancer.

The principle behind this microfluidic device is that most cancer cells are larger and less deformable than blood cells, making them less likely to transverse through the microfluidic channels, hence being retained in the device filtering areas; while most blood cells pass through. In this preliminary study, it was evident the correlation between cell size and deformability and the capture efficiency, since largest and less deformable cells, like SW480 cells, were captured with high sensitivity (approximately 70 % sensitivity) by the microfluidic device. In addition, the optimal flow rate was also determined in this study, 100 μL/min, to be applied in metastatic colorectal cancer patients in future clinical studies.

Moreover, a consistent cell capture ability of the device was demonstrated since changing the spiked cell target, showed no relevant influence of the capture efficiency, which suggest that capture efficiency will be maintained equal in samples with low or high CTC content.

In addition to allowing a fast, sensitive and highly efficient CTC capture, the RUBYchip™ also enables the identification of tumour cells, which are mainly based on biological properties using antibodies against tumour-associated antigen (positive marker) and the common leucocytes antigen (negative marker). In this study, Cytokeratin and Vimentin were used to identify CTCs in metastatic CRC setting, since several reports have already demonstrated that the presence of Vimentin is strongly associated with worse prognosis compared to those with the expression of CK alone[101,102]. Using three-color immune-fluorescent staining, relatively high definition images of immune-stained colorectal cancer cell lines were obtained. All CRC cell lines were positive for Cytokeratin, but only SW480 cells were Vimentin-positive. Using this latter cells, different biological samples from healthy volunteers were spiked and processed in the device and subsequently stained with the testing antibodies. In this study, we were able to find a very specific CD45 (Santa Cruz) antibody to be further applied in future clinical studies. Regarding Cytokeratin, both antibodies used against this biomarker had a good

performance, however still present associated limitations that were not immediately overcome, but subsequent optimization works and dedicated specific bioimaging and analysis equipment would be able to solve. For that reason, to progress into future clinical studies an equipment specifically developed for bioimaging of CTCs and with a high throughput automatized software for CTC analysis is ideal.

In this study, different CTC cell populations were also detected in metastatic colorectal cancer patients, namely $CK^+/Vimentin^+/CD45^-$, $CK^-/Vimentin^+/CD45^-$, in addition to $CK^+/Vimentin^-/CD45^-$, using the RUBYchip™. Those cells co-expressing CK and Vimentin may be CTCs undergoing EMT, hence future studies using clinical samples should be conducted to determine whether CTCs with mesenchymal phenotype (Vimentin-positive tumour cells) could be correlated to clinical pathophysiological features and outcomes.

The characterization of CTCs at the molecular level will facilitate personalised medicine since it will allow the analysis of pharmacodynamic and predictive biomarkers, as well as the analysis of drug sensitivity biomarkers and inherited or acquired drug therapy resistance[103]. Therefore, as future perspectives, we aim to further validate the optimal parameters found in this study, in larger longitudinal clinical studies with a very well-defined cohort of metastatic colorectal cancer patients to evaluate the prognostic value and disease monitoring potential of the RUBYchip™.

Additionally, comparative studies, regarding the CTCs capture and enumeration, with the standard technologies could bring valuable information in terms of sensitivity and specificity of the microfluidic device. This study also gives the opportunity for future CTC expansion studies with the recovery of this events from cancer patients' blood and, subsequent cell culturing in order to proceed with drug test screening, or even the supervision of a tumour's drug susceptibility dynamic patterns.

Notwithstanding the limitations currently being addressed, CTCs appear as one of the most promising and versatile biomarkers in translational oncology, having the potential to become, in the near future, an important landmark of precision medicine.

6. Bibliography

1. HOWE, Lady. A matter of life and death. *Economist*. (2009).392(8642):19-30.
2. HARVEY L, ARNOLD B, LAWRENCE Z, et al. *Molecular Cell Biology*. 4th ed. W. H. Freeman and Company.(2000.)https://www.ncbi.nlm.nih.gov/books/NBK21475/
3. HANAHAN D, WEINBERG RA. The hallmarks of Cancer. *Cell*. (2000).100(1):57-70. doi:https://doi.org/10.1016/S0092-8674(00)81683-9
4. HANAHAN D, WEINBERG RA. Hallmarks of cancer: The next generation. *Cell*. (2011).144(5):646-674. doi:10.1016/j.cell.2011.02.013
5. HORNE SD, POLLICK SA, HENG HHQ. Evolutionary mechanism unifies the hallmarks of cancer. *Int J Cancer*. (2015).136(9):2012-2021.doi:10.1002/ijc.29031
6. CANCER RESEARCH UK. https://www.cancerresearchuk.org/health-professional/cancer-statistics/worldwide-cancer
7. THE GLOAL CANCER OBSERVATORY W. Globocan 2018 - Portugal. *Int Agency Res Cancer*. 2019;270:2018-2019. http://gco.iarc.fr/today/data/factsheets/populations/620-portugal-fact-sheets.pdf.
8. SOCIETY AC. Colorectal Cancer Facts & Figures 2017-2019 ; 1–40. Available from: https://www.cancer.org/content/dam/cancer-org/research/cancer-facts-and-statistics/colorectal-cancer-facts-and-figures/colorectal-cancer-facts-and-figures-2017-2019.pdf. *Centers Dis Control Prev Behav Risk Factor Surveill Syst 2014 Public use data file Color Cancer Screen*. Published online 2017. https://www.mendeley.com/viewer/?fileId=446a0f98-7242-86a5-07ff-be4c6c8cd11c&documentId=3b9629ab-fc85-3cb8-9607-7468ed4f76a7
9. PETRELLI F, TOMASELLO G, BORGONOVO K, et al. Prognostic Survival Associated With Left-Sided vs Right-Sided Colon Cancer: A Systematic Review and Meta-analysis. *JAMA Oncol*. (2017).3(2):211-219. doi:10.1001/jamaoncol.2016.4227.
10. MÁRMOL I, SÁNCHEZ-DE-DIEGO C, DIESTE AP, CERRADA E, YOLDI MJR. Colorectal carcinoma: A general overview and future perspectives in colorectal cancer. *Int J Mol Sci*. 2017;18(1). doi:10.3390/ijms18010197
11. HARSHMAN M, ALDOORI W. Diet and colorectal cancer: Review of the evidence. *Can Fam Physician*. (2007).53(11):1913-1920.
12. SINGH PN, FRASER GE. Dietary risk factors for colon cancer in a low-risk population. *Am J Epidemiol*. (1998).148(8):761-774.

doi:10.1093/oxfordjournals.aje.a009697

13. BALLINGER AB, ANGGIANSAH C. Colorectal cancer. *Br Med J*. (2007).335(7622):715-718. doi:10.1136/bmj.39321.527384.BE
14. SIMON K. Colorectal cancer development and advances in screening. *Clin Interv Aging*. (2016).11:967-976. doi:10.2147/CIA.S109285
15. DAS V, KALITA J, PAL M. Predictive and prognostic biomarkers in colorectal cancer: A systematic review of recent advances and challenges. *Biomed Pharmacother*. (2017).87:8-19. doi:10.1016/j.biopha.2016.12.064
16. GASTROENTEROL WJ. World Journal of. (2017).9327(28).
17. LIN OS, KOZAREK RA, CHA JM. Impact of Sigmoidoscopy and Colonoscopy on Colorectal Cancer Incidence and Mortality: An Evidence-Based Review of Published Prospective and Retrospective Studies. *Intest Res*. (2014).12(4):268. doi:10.5217/ir.2014.12.4.268
18. NIEDERmMAIER T, Weigl K, HOFFMEISTER M, BRENNER H. Flexible sigmoidoscopy in colorectal cancer screening: implications of different colonoscopy referral strategies. *Eur J Epidemiol*. (2018).33(5):473-484. doi:10.1007/s10654-018-0404-x
19. JACQUES FF, ISABELLE S, R. D, et al. Colon and Rectum Cancer Staging. *Am Cancer Soc*. Published online (2009).1.
20. NATIONAL CANCER INSTITUTE SURVEILLANCE, Epidemiology and ER program. Cancer Stat Facts: Colorectal Cancer. Published 2018. https://seer.cancer.gov/statfacts/html/colorect.html
21. RIIHINAKI M, HEMMINKI A, SUNDQUIST J, HEMMINKI K. Patterns of metastasis in colon and rectal cancer. *Sci Rep*. (2016). 6:1-9. doi:10.1038/srep29765
22. KASTRINOS F, SYNGAL S. Inherited Colorectal Cancer Syndromes. *Cancer J*. (2012).17(6):405-415. doi:10.1097/PPO.0b013e318237e408
23. LYNCH HT, CHAPELLE A. Hereditary Colorectal Cancer. *N Engl J Med*. (2003).348(10):919-932. doi:10.1056/NEJMra012242.
24. CUYLE PJ, PRENEN H. Current and future biomarkers in the treatment of colorectal cancer. *Acta Clin Belgica Int J Clin Lab Med*. (2017).72(2):103-115. doi:10.1080/17843286.2016.1262996
25. FEARON ER, VOLGELSTEIN B. A Genetic Model for Colorectal Tumorigenesis. *Cell*. (1990).61(5):759-767. doi:10.1016/0092-8674(90)90186-i
26. TARIQ K, GHIAS K. Colorectal cancer carcinogenesis: a review of mechanisms.

Cancer Biol Med. (2016).13(1):120-135. doi:10.28092/j.issn.2095-3941.2015.0103

27. WORLD HEALTH ORGANIZATION & International Programme on Chemical Safety. Biomarkers in risk assessment : validity and validation. http://www.inchem.org/documents/ehc/ehc/ehc222.htm
28. ALVES Martins BA, de BULHÕES GF, CAVALCANTI IN, MARTINS MM, DE OLIVEIRA PG, MARTINS AMA. Biomarkers in Colorectal Cancer: The Role of Translational Proteomics Research. *Front Oncol*. (2019). 1-11. doi:10.3389/fonc.2019.01284
29. LEMECH C, ARKENAU HT. Biomarkers in advanced colorectal cancer: Challenges in translating clinical research into practice. *Cancers (Basel)*. (2011). 3(2):1844-1860. doi:10.3390/cancers3021844
30. LECH G, SŁOTWIŃSKI R, SŁODKOWSKI M, KRASNODEBSKI IW. Colorectal cancer tumour markers and biomarkers: Recent therapeutic advances. *World J Gastroenterol*. (2016).22(5):1745-1755. doi:10.3748/wjg.v22.i5.1745
31. VACANTE M, BORZI AM, BASILE F, BIONDI A. Biomarkers in colorectal cancer: Current clinical utility and future perspectives. *World J Clin Cases*. (2018). 6(15):869-881. doi:10.12998/wjcc.v6.i15.869
32. BOUTIN AT, LIAO WT, WANG M, et al. Oncogenic Kras drives invasion and maintains metastases in colorectal cancer. *Genes Dev*. (2017).31(4):370-382. doi:10.1101/gad.293449.116
33. JIANG WQ, FU FF, LI YX, et al. Molecular biomarkers of colorectal cancer: Prognostic and predictive tools for clinical practice. *J Zhejiang Univ Sci B*. 2012;13(9):663-675. doi:10.1631/jzus.B1100340
34. THIERY JP, SLEEMAN JP. Complex networks orchestrate epithelial-mesenchymal transitions. *Nat Rev Mol Cell Biol*. (2006).7(2):131-142. doi:10.1038/nrm1835
35. NANTAJIT D, LIN D, LI J. The network of epithelial-mesenchymal transition: potential new targets for tumor resistance. *J Cancer Res Clin Oncol*. (2014).141(10):1697-1713. doi:10.1007/s00432-014-1840-y
36. OLEA M, ZUNIGA MD, MENDONZA MA, et al. Extracellular-signal regulated kinase: A central molecule driving epithelial–mesenchymal transition in cancer. *Int J Mol Sci*. (2019).20(12):1-32. doi:10.3390/ijms20122885
37. DAS V, BHATTACHARYNA S, CHIKKAPUTTAIH C, HAZRA S, Pal M. The basics of epithelial–mesenchymal transition (EMT): A study from a structure, dynamics, and functional perspective. *J Cell Physiol*. (2019).234(9):14535-14555.

doi:10.1002/jcp.28160

38. VU T, DATTA PK. Regulation of EMT in colorectal cancer: A culprit in metastasis. *Cancers (Basel)*. (2017)9(12):1-22. doi:10.3390/cancers9120171
39. YAN X, YAN L, LIU S, SHAN Z, TIAN Y, JIN Z. N-cadherin, a novel prognostic biomarker, drives malignant progression of colorectal cancer. *Mol Med Rep*. (2015).12(2):2999-3006. doi:10.3892/mmr.2015.3687
40. MITTAL V. Epithelial Mesenchymal Transition in Tumor Metastasis. *Annu Rev Pathol Mech Dis*. (2018).13(1):395-412. doi:10.1146/annurev-pathol-020117-043854
41. HARRIS LA, BEIK S, OZAWA PMM, JIMENEZ L, WEAVER AM. Modeling heterogeneous tumor growth dynamics and cell–cell interactions at single-cell and cell-population resolution. *Curr Opin Syst Biol*. (2019).24-34. doi:10.1016/j.coisb.2019.09.005
42. RUSSANO M, NAPOLITANO A, RIBELLI G, et al. Liquid biopsy and tumor heterogeneity in metastatic solid tumors: The potentiality of blood samples. *J Exp Clin Cancer Res*. (2020).39(1):1-13. doi:10.1186/s13046-020-01601-2
43. JOLLY MK, CELIÀ-TERRASSE T. Dynamics of Phenotypic Heterogeneity Associated with EMT and Stemness during Cancer Progression. *J Clin Med*. (2019).8(10):1542. doi:10.3390/jcm8101542
44. HOFMAN P, POPPER HH. Pathologists and liquid biopsies: to be or not to be? *Virchows Arch*. (2016).469(6):601-609. doi:10.1007/s00428-016-2004-z
45. ILIÉ M, HOFMAN P. Pros: Can tissue biopsy be replaced by liquid biopsy? *Transl Lung Cancer Res*. (2016).5(4):420-423. doi:10.21037/tlcr.2016.08.06
46. BARDELLI A, PANTEL K. Liquid Biopsies, What We Do Not Know (Yet). *Cancer Cell*. (2017).31(2):172-179. doi:10.1016/j.ccell.2017.01.002
47. BEST MG, SOL N, KOOI I, et al. RNA-Seq of Tumor-Educated Platelets Enables Blood-Based Pan-Cancer, Multiclass, and Molecular Pathway Cancer Diagnostics. *Cancer Cell*. (2015).28(5):666-676. doi:10.1016/j.ccell.2015.09.018
48. PALMIROTTA R, LOVERO D, CAFFORIO P, et al. Liquid biopsy of cancer: a multimodal diagnostic tool in clinical oncology. *Ther Adv Med Oncol*. (2018).10:1-24. doi:10.1177/1758835918794630
49. KWAPISZ D. The first liquid biopsy test approved. Is it a new era of mutation testing for non-small cell lung cancer? *Ann Transl Med*. (2017). 5(3):1-7. doi:10.21037/atm.2017.01.32

50. NORCIC G. Liquid biopsy in colorectal cancer-current status and potential clinical applications. *Micromachines*. (2018).9(6). doi:10.3390/mi9060300
51. NORMANNO N, CERVANTES A, CIARDIELLO F, DE LUCA A, Pinto C. The liquid biopsy in the management of colorectal cancer patients: Current applications and future scenarios. *Cancer Treat Rev*. (2018)70:1-8. doi:10.1016/j.ctrv.2018.07.007
52. SASTRE J, MAESTRO ML, PUENTE J, et al. Circulating tumor cells in colorectal cancer: Correlation with clinical and pathological variables. *Ann Oncol*. (2008).19(5):935-938. doi:10.1093/annonc/mdm583
53. BURZ C, POP V-V, BUIGA R, et al. Circulating tumor cells in clinical research and monitoring patients with colorectal cancer. *Oncotarget*. (2018).9(36):24561-24571. doi:10.18632/oncotarget.25337
54. WANG JY, HSIEH JS, CHANG MY, et al. Molecular detection of APC, K-ras, and p53 mutations in the serum of colorectal cancer patients as circulating biomarkers. *World J Surg*. (2004).28(7):721-726. doi:10.1007/s00268-004-7366-8
55. TIE J, WANG Y, TOMASETTI C, et al. cancer. (2017).8(346). doi:10.1126/scitranslmed.aaf6219.Circulating
56. CROWLEY E, DI NICOLANTONIO F, LOUPAKIS F, BARDELLI A. Liquid biopsy: Monitoring cancer-genetics in the blood. *Nat Rev Clin Oncol*. (2013).10(8):472-484. doi:10.1038/nrclinonc.2013.110
57. CHEN L, BODE AM, DONG Z. Circulating tumor cells: Moving biological insights into detection. *Theranostics*. (2017).7(10):2606-2619. doi:10.7150/thno.18588
58. ENGELL H. Cancer cells in the circulating blood; a clinical study on the occurrence of cancer cells in the peripheral blood and in venous blood draining the tumour area at operation. *Acta Chir Scand*. (1955).201:1–70.
59. LEATHER AJM, GALLEGOS NC, KOCJAN G, et al. Detection and enumeration of circulating tumour cells in colorectal cancer. *Br J Surg*. (1993).80(6):777-780. doi:10.1002/bjs.1800800643
60. STEINERT G, SCHOLCH S, KOCH M, WEITZ J. Biology and significance of circulating and disseminated tumour cells in colorectal cancer. *Langenbeck's Arch Surg*. (2012).397(4):535-542. doi:10.1007/s00423-012-0917-9
61. VALASTYAN S, WEINBERG RA. Tumor metastasis: Molecular insights and evolving paradigms. *Cell*. (2011).147(2):275-292. doi:10.1016/j.cell.2011.09.024
62. MICALIZZI DS, MAHESWARAN S, HABER DA. A conduit to metastasis: Circulating tumor cell biology. *Genes Dev*. (2017).31(18):1827-1840.

doi:10.1101/gad.305805.117

63. HUANG MY, TSAI HL, HUANG JJ, WANG JY. Clinical implications and future perspectives of circulating tumor cells and biomarkers in clinical outcomes of colorectal cancer. *Transl Oncol*. (2016).9(4):340-347. doi:10.1016/j.tranon.2016.06.006
64. WANG H, LIN S, UEN Y, WANG J. Molecular detetction of circulating tumor cells in colorectal cancer patients: from laboratory to clinical implication. *Fooyin J Heal Sci*. (2009).1(1):2-10.
65. GAZZANIGA P, RAIMONDI C, GRADILONE A, et al. Circulating tumor cells in metastatic colorectal cancer: Do we need an alternative cutoff? *J Cancer Res Clin Oncol*. (2013).139(8):1411-1416. doi:10.1007/s00432-013-1450-0
66. COHEN SJ, PUNT CJA, IANNOTTI N, et al. Prognostic significance of circulating tumor cells in patients with metastatic colorectal cancer. *Ann Oncol*. (2009).20(7):1223-1229. doi:10.1093/annonc/mdn786
67. COHEN SJ, PUNT CJA, IANNOTTI N, et al. Relationship of circulating tumor cells to tumor response, progression-free survival, and overall survival in patients with metastatic colorectal cancer. *J Clin Oncol*. (2008).26(19):3213-3221. doi:10.1200/JCO.2007.15.8923
68. LIM SH, BECKER TM, CHUA W, et al. Circulating tumour cells and circulating free nucleic acid as prognostic and predictive biomarkers in colorectal cancer. *Cancer Lett*. (2014).346(1):24-33. doi:10.1016/j.canlet.2013.12.019
69. GAZZANIGA P, GRADILONE A, PETRACCA A, et al. Molecular markers in circulating tumour cells from metastatic colorectal cancer patients. *J Cell Mol Med*. (2010).14(8):2073-2077. doi:10.1111/j.1582-4934.2010.01117.x
70. TOL J, KOOPMAN M, MILLER MC, et al. Circulating tumour cells early predict progression-free and overall survival in advanced colorectal cancer patients treated with chemotherapy and targeted agents. *Ann Oncol*. (2009).21(5):1006-1012. doi:10.1093/annonc/mdp463
71. ALIX-PANABIERES C, PANTEL K. Circulating tumor cells: Liquid biopsy of cancer. *Clin Chem*. (2013).59(1):110-118. doi:10.1373/clinchem.2012.194258
72. MAMDOUHI T, TWONEY JD, MCSWEENEY KM, ZHANG B. Fugitives on the run: circulating tumor cells (CTCs) in metastatic diseases. *Cancer Metastasis Rev*. (2019).38(1-2):297-305. doi:10.1007/s10555-019-09795-4
73. YU M, STOTT S, TONER M, MAHESWARAN S, HABER DA. Circulating tumor cells:

Approaches to isolation and characterization. *J Cell Biol*. (2011).192(3):373-382. doi:10.1083/jcb.201010021

74. WICHA MS, HAYES DF. Circulating Tumor Cells: Not All Detected Cells Are Bad and Not All Bad Cells Are Detected. *J Clin Oncol*. (2011).29(12):1508-1511. doi:10.1200/JCO.2010.34.0026.
75. ANDREE KC, VAN DALUM G, TERSTAPPEN LW. Challenges in circulating tumor cell detection by the CellSearch system. *Mol Oncol*. (2016).10(3):395-407. doi:10.1016/j.molonc.2015.12.002
76. MILLNER LM, LINDER MW, VALDES R. Circulating tumor cells: A review of present methods and the need to identify heterogeneous phenotypes. *Ann Clin Lab Sci*. (2013).43(3):295-304.
77. ESMAEILSABZALI H, BEISCHLAG TV, COX ME, PARAMESWARAN AM, PARK EJ. Detection and isolation of circulating tumor cells: Principles and methods. *Biotechnol Adv*. (2013).31(7):1063-1084. doi:10.1016/j.biotechadv.2013.08.016
78. ALLARD WJ, MATERA J, MILLER MC, et al. Tumor cells circulate in the peripheral blood of all major carcinomas but not in healthy subjects or patients with nonmalignant diseases. *Clin Cancer Res*. (2004).10(20):6897-6904. doi:10.1158/1078-0432.CCR-04-0378
79. DONG Y, SKELLEY AM, MERDECK KD, et al. Microfluidics and circulating tumor cells. *J Mol Diagnostics*. (2013).15(2):149-157. doi:10.1016/j.jmoldx.2012.09.004
80. MARRINUCCI D, BETHEL K, BRUCE RH, et al. Case study of the morphologic variation of circulating tumor cells. *Hum Pathol*. (2007).38(3):514-519. doi:10.1016/j.humpath.2006.08.027
81. MYUNG JH, HONG S. Microfluidic devices to enrich and isolate circulating tumor cells. *Lab Chip*. (2015).15(24):4500-4511. doi:10.1039/c5lc00947b
82. NAGRATH S, SEQUIST L, BELL D, et al. Isolation of rare circulating tumour cells in cancer patients by microchip technology. *Nature*. (2007).450:1235-1239.
83. XU L, MAO X, IMRALI A, SYED F, MUTSVANGWA K. Optimization and Evaluation of a Novel Size Based Circulating Tumor Cell Isolation System. Published online (2015).1-23. doi:10.1371/journal.pone.0138032
84. RENIER C, PAO E, CHE J, et al. Label-free isolation of prostate circulating tumor cells using Vortex micro fl uidic technology. *npj Precis Oncol*. (2017). 1-10. doi:10.1038/s41698-017-0015-0
85. RIBEIRO-SAMY S, OLIVEIRA MI, PEREIRA-VEIGA T, et al. Fast and efficient

microfluidic cell filter for isolation of circulating tumor cells from unprocessed whole blood of colorectal cancer patients. *Sci Rep*. (2019).9(1):1-12. doi:10.1038/s41598-019-44401-1

86. NEVES M, AZEVEDO R, LIMA L, et al. Exploring sialyl-Tn expression in micro fl uidic-isolated circulating tumour cells : A novel biomarker and an analytical tool for precision oncology applications. (2019).49:77-87. doi:10.1016/j.nbt.2018.09.004
87. AZEVEDO R, SOARES J, PEIXOTO A, et al. Circulating tumor cells in bladder cancer: Emerging technologies and clinical implications foreseeing precision oncology. *Urol Oncol Semin Orig Investig*. (2018).36(5):221-236. doi:10.1016/j.urolonc.2018.02.004
88. VAICKUS LJ, TAMBOURET RH. Young investigator challenge: The accuracy of the nuclear-to-cytoplasmic ratio estimation among trained morphologists. *Cancer Cytopathol*. (2015).123(9):524-530. doi:10.1002/cncy.21585
89. XIA Y, Wan Y, HAO S, et al. Nucleus of Circulating Tumor Cell Determines Its Translocation Through Biomimetic Microconstrictions and Its Physical Enrichment by Microfiltration. *Small*. (2018).14(44):1-11. doi:10.1002/smll.201802899
90. WONG C, WONG V, CHAN C, et al. Identification of 5-fluorouracil response proteins in colorectal carcinoma cell line SW480 by two-dimensional electrophoresis and MALDI-TOF mass spectrometry. *Oncol Rep*. (2008).20:89-98.
91. LENAERTS K, BOUWMAN FK, LAMERS WH, RENES J, MARIMAN EC. Comparative proteomic analysis of cell lines and scrapings of the human intestinal epithelium. *BMC Genomics*. (2007).8:1-14. doi:10.1186/1471-2164-8-91
92. TOIYAMA Y, YASUDA H, SAIGUSA S, et al. Increased expression of slug and vimentin as novel predictive biomarkers for lymph node metastasis and poor prognosis in colorectal cancer. *Carcinogenesis*. (2013).34(11):2548-2557. doi:10.1093/carcin/bgt282
93. MCINROY L, MÃÃTÃ A. Down-regulation of vimentin expression inhibits carcinoma cell migration and adhesion. *Biochem Biophys Res Commun*. (2007).360(1):109-114. doi:10.1016/j.bbrc.2007.06.036
94. PODOR TJ, SINGTH D, CHINDEMI P, et al. Vimentin exposed on activated platelets and platelet microparticles localizes vitronectin and plasminogen activator inhibitor complexes on their surface. *J Biol Chem*. (2002).277(9):7529-7539.

doi:10.1074/jbc.M109675200

95. MOISAN E, GIRARD D. Cell surface expression of intermediate filament proteins vimentin and lamin B 1 in human neutrophil spontaneous apoptosis . *J Leukoc Biol*. (2006).79(3):489-498. doi:10.1189/jlb.0405190
96. SU L, PAN P, YAN P, et al. Role of vimentin in modulating immune cell apoptosis and inflammatory responses in sepsis. *Sci Rep*. (2019).9(1):1-14. doi:10.1038/s41598-019-42287-7
97. COUMANS FA, DOGGEN CJM, ATTARD G, DE BONO JS, TERSTAPPEN L. All circulating EpCAM+CK+CD45-objects predict overall survival in castration-resistant prostate cancer. *Ann Oncol*. (2010).21(9):1851-1857. doi:10.1093/annonc/mdq030
98. CHE J, YU V, DHAR M, et al. Classification of large circulating tumor cells isolated with ultra-high throughput microfluidic Vortex technology. *Oncotarget*. (2016).7(11):12748-12760. doi:10.18632/oncotarget.7220
99. VAN DER TOOM EE, VERDONE JE, GORIN MA, PIENTA KJ. Technical challenges in the isolation and analysis of circulating tumor cells. *Oncotarget*. (2016;).(38):62754-62766. doi:10.18632/oncotarget.11191
100. GRIFFITHS G, LUCOCQ JM. Antibodies for immunolabeling by light and electron microscopy: Not for the faint hearted. *Histochem Cell Biol*. (2014).142(4):347-360. doi:10.1007/s00418-014-1263-5
101. GRADILLONE A, NASO G, RAIMONDI C, et al. Circulating tumor cells (CTCs) in metastatic breast cancer (MBC): Prognosis, drug resistance and phenotypic characterization. *Ann Oncol*. (2011).22(1):86-92. doi:10.1093/annonc/mdq323
102. GAO W, YUAN H, JING F, et al. Analysis of circulating tumor cells from lung cancer patients with multiple biomarkers using high-performance size-based microfluidic chip. *Oncotarget*. (2017).8(8):12917-12928. doi:10.18632/oncotarget.14203
103. KREBS MG, HOU JM, WARD TH, BLACKHAL FH, DIVE C. Circulating tumour cells: Their utility in cancer management and predicting outcomes. *Ther Adv Med Oncol*. (2010).2(6):351-365. doi:10.1177/1758834010378414